energies

MDPI

Review

A Review of Biomass Thermal Analysis, Kinetics and Product Distribution for Combustion Modeling: From the Micro to Macro Perspective

João Silva [1,2,*], Senhorinha Teixeira [2] and José Teixeira [1]

[1] MEtRICs Research Centre, University of Minho, 4800-058 Guimarães, Portugal; jt@dem.uminho.pt
[2] ALGORITMI Research Centre/LASI, University of Minho, 4800-058 Guimarães, Portugal; st@dps.uminho.pt
* Correspondence: js@dem.uminho.pt

Abstract: Driven by its accessibility, extensive availability, and growing environmental consciousness, solid biomass has emerged as a viable alternative to enhance the diversity of renewable energy sources for electricity generation. To understand the phenomena involved in solid biomass conversion, it is necessary not only to understand the stages of the biomass combustion process but also to understand specifically the kinetics of the reaction and the release of the volatiles. The present work presents an overview of the existing literature on several topics related to the biomass combustion process, its characterization, as well as strategies to develop simple and effective models to describe biomass conversion with a view to the future development of numerical simulation models. Since the focus of most of the investigations is the development of a numerical model, a summary and identification of the different model assumptions and problems involved in thermal analysis experiments are presented. This literature review establishes the significance and credibility of the research, providing the main concepts and assumptions with a critique on their validity. Hence, this work provides specific contributions from a multi-scale perspective which can further be extended to provide insights into the design and optimization of biomass combustion technologies, such as boilers and furnaces.

Keywords: biomass; combustion; kinetics; macro thermogravimetric analysis; thermal analysis

Citation: Silva, J.; Teixeira, S.; Teixeira, J. A Review of Biomass Thermal Analysis, Kinetics and Product Distribution for Combustion Modeling: From the Micro to Macro Perspective. *Energies* **2023**, *16*, 6705. https://doi.org/10.3390/en16186705

Academic Editor: Dimitrios Kalderis

Received: 2 August 2023
Revised: 5 September 2023
Accepted: 11 September 2023
Published: 19 September 2023

1. Introduction

Energy demand has increased over the years due to population growth and industrial and socio-economic developments, cornerstones of human civilization. As fossil fuels have been the backbone of energy supply worldwide, they are linked with climate change and global warming. Besides the protection of the environment, the depletion of fossil fuel resources is an important aspect that needs to be overcome. Consequently, using alternative energy sources to reduce environmental problems and strain on limited supply is currently a primary concern. As an alternative clean energy source, biomass appears to be a very interesting option as it is considered a sustainable, renewable, and CO_2-neutral energy source [1], even though this has been seriously debated recently [2–6]. Furthermore, its abundance and availability not depending on weather conditions make this resource an attractive and valuable alternative for energy supply in both domestic and industrial sectors. Banja et al. [7] noted that biomass is the main contributor to EU renewable energy markets and due to its lower carbon footprint, has a significant contribution to low-carbon economy which results in its key role within the EU policy in the support for renewable energy sources. Furthermore, the International Energy Agency Roadmap—Net Zero Emissions by 2050—identifies bioenergy as an important source of energy, projected to represent 18% of the total energy supply in 2050,playing a key role in the transition toward a carbon-neutral society [8]. This number considers the direct replacement of fossil fuels and, indirectly, the counterbalance emissions by coupling the use of bioenergy with carbon capture and

storage. In 2019, the replacement of fossil fuels with biomass avoided 290 $MtCO_2eq$ emissions, equivalent to approximately 8% of the EU27 GHG emissions [9].

Nowadays, biomass thermochemical conversion can be categorized into several main types, including combustion, pyrolysis, gasification, and hydrothermal processes. These processes have gained significant interest in recent years due to their potential to produce renewable energy and/or bio-based products while reducing greenhouse gas emissions. Each one has different characteristics and results in different products [10], combustion being the oldest and most mature technology for the production of heat and power. Additionally, the main route for providing renewable heat is solid biomass combustion, typically in grate-fired boilers. The applications of biomass combustion cover a wide range from domestic equipment with dozens of kW to district heating, dedicated, or combined heat and power plants with up to hundreds of MW of installed capacity. The successive climate targets for 2020, 2030, and 2050 have progressively reduced gas emissions targets up to 80% by increasing the share of renewable energy in the energy mix [11]. Nonetheless, there are countries like Portugal, with regard to the biomass sector, that only promote the development of new small co-generation biomass plants (up to 15 MW [12]). The low efficiency of dedicated large-scale biomass plants certainly discourages support for them.

The low efficiency is related to the complexity of the biomass combustion process, its instability, and the non-utilization of the available thermal energy for other purposes. Biomass combustion involves simultaneous multiphase fluid flow, chemical reactions, heat (convection and radiation), and mass transfer [13]. Due to this complex and irregular process, there are various operational problems inside an industrial boiler. Additionally, the pollutant emission limit is often exceeded.

In this regard, in order to give scientific insight into this phenomenon, experiments and Computational Fluid Dynamics (CFD) modeling are complementary tools for the development of thermal analysis, in-depth study of each reaction, and prediction of the gas flow to further anticipate problems that can occur during the combustion phase. The understanding of the processes in the fuel bed is rather limited, as it is difficult to obtain information through direct measurements because of the limited physical and optical accessibility inside a grate-fired boiler. Therefore, experiments at a reduced scale are necessary. Hence, this work presents an overview of the state-of-the-art of the literature concerning the thermal analysis, kinetics, and volatiles compounds involved in solid biomass conversion with a particular focus on the further development of simple and accurate CFD models.

2. Thermal Analysis in Biomass Combustion

As it is impossible to maintain repeatable and fully controlled conditions, and to monitor all the dynamics involved in lab-scale experiments, it becomes necessary to perform investigations at a small scale. This should be adequate to provide a controlled environment, and large enough to define realistic conditions. Furthermore, due to the design and operation of industrial biomass boilers, there is a need to model the combustion to further determine their key operating and design parameters. Moreover, biomass combustion in grate-fired boilers can be described as a series of reactions, which begins at a relatively small scale.

As represented in Figure 1, a comprehensive understanding of devolatilization is fundamental to the conversion process. In order to completely characterize this stage, the kinetics of the reaction and the determination of the volatiles released are essential. The study of biomass combustion behavior and the kinetics of the solid-state reactions have been developed through fundamental thermal analysis methods. According to the International Confederation for Thermal Analysis and Calorimetry (ICTAC), thermal analysis is referred to as a group of techniques where a property of the sample is monitored against time and/or temperature and, consequently, the change of the sample in terms of its weight is measured as a result of an imposed temperature profile in a specified atmosphere [14]. In previous work, thermogravimetric analysis (TGA) is the most common thermoanalytical technique

used for solid-phase thermal degradation studies and for kinetic measurements [15,16], while analysis of the gaseous release process and the heat and mass transfer effects can be evaluated using the same technique but at a larger scale, which is commonly known as macro-TGA [17].

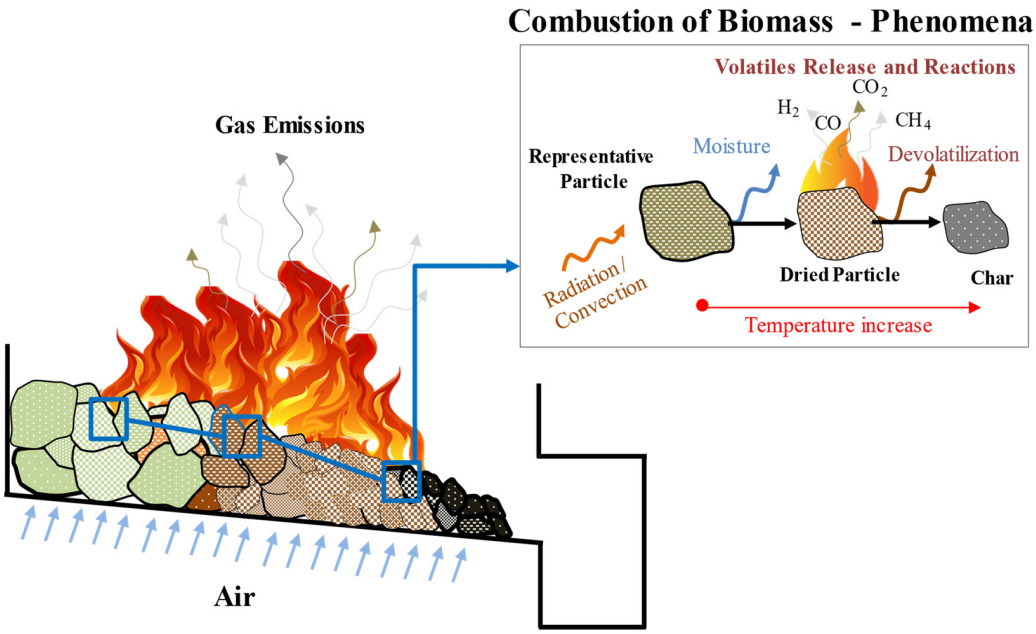

Figure 1. An overview of the phenomena occurring during the multi-scale biomass combustion process.

2.1. Thermogravimetric Analysis

As biomass combustion is a complex process [18], it is important to understand the physical and chemical processes involved at the particle level to enable proper understanding [19,20]. TGA is a powerful tool used to study the devolatilization rate during the biomass combustion process and obtain important parameters which are essential in characterizing and understanding its behavior [21,22]. TGA is widely implemented for investigating and comparing thermal degradation events and kinetics during the combustion of solid materials such as coal and biomass [23]. The decrease in mass is measured under controlled conditions while the thermal process is taking place, as the temperature increases with time. Consequently, information about the thermal conversion dependency on temperature will be obtained at the particle scale. According to the search results from the Web of Science Database using the keywords "thermogravimetric analysis" and "biomass", there has been a growing trend around biomass and the application of TGA to biomass in scientific journals since 2000. Figure 2 presents the annual number of publications from 2000 to 2021, which highlights the use and importance of TGA to investigate the thermal decomposition of biomass.

A thermogravimetric analyzer consists of a sample pan that is supported by a precision balance placed in a furnace where the heating rate and environment can be controlled. Time, temperature, and weight are the three variables continuously measured and recorded during the TGA experiment. Taking the first derivative of such recorded data, known as derivative thermogravimetry (DTG), important parameters of thermal behavior characterization are provided. These key parameters are initial decomposition (T_{in}), peak (T_{max}), and burnout (T_b) temperatures. T_{in} corresponds to the beginning of the weight loss, and it is defined as the temperature at which the rate of weight loss reaches 1%/min after the initial moisture loss peak in the DTG profile. T_{max} is the point at which the maximum reaction rate occurs. T_b is identified when the last peak comes to the end and the temperature at which the sample is completely oxidized. It is taken as the point immediately before the reaction ceases when the rate of weight loss is down to 1%/min [24]. All this information allows for

the thermal decomposition characterization of biomass samples and, in particular, the last two characteristic temperatures are important fuel parameters, especially in establishing the residence time in the combustion chamber. The experimental procedure and the most important points are illustrated in Figure 3.

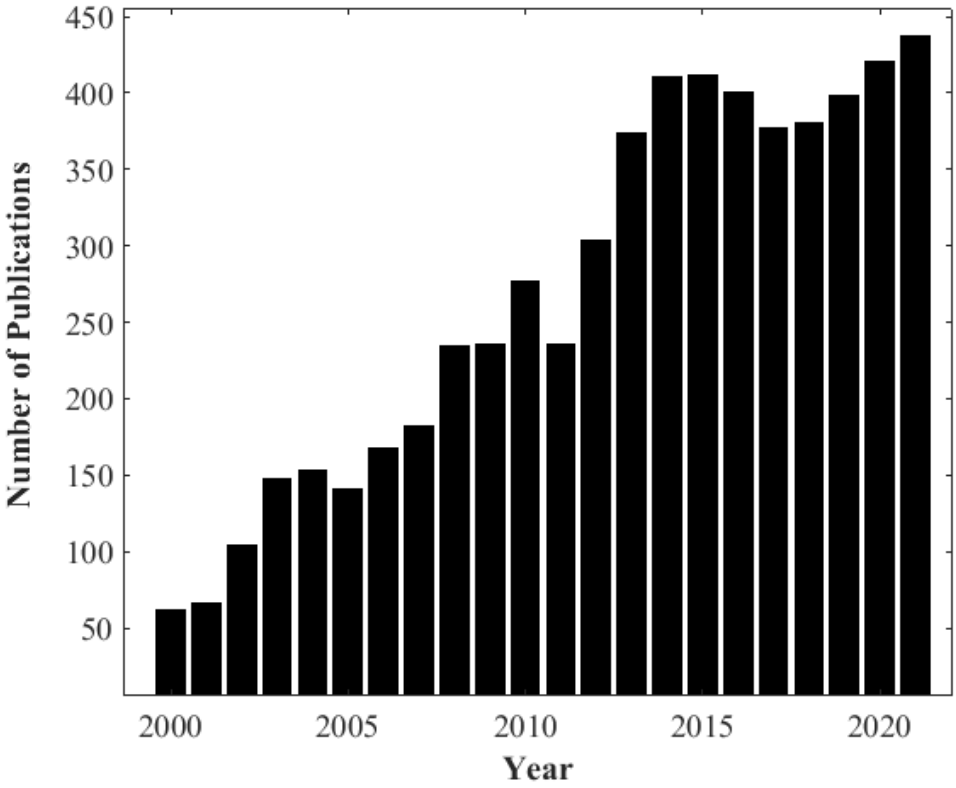

Figure 2. Number of annual publications from 2000 to the present on thermogravimetric analysis, TGA, and biomass: Data Source: results from Web of Knowledge Database.

The shape of the thermogravimetric curves (TG) and DTG curves is dependent on several factors, including the type of biomass; atmosphere and its flow rate; the heating program which includes the heating rate and the final temperature; initial mass; and the particle size of the fuel [26]. These constitute the main factors that affect the TG and that will determine the characteristic thermal decomposition behavior. The initial mass and particle size should be as small as possible to avoid the effect of heat and mass transfer limitations [11,27]. Regarding the atmosphere, there are two options to be considered: the oxidative or inert. An oxidative atmosphere greatly affects the devolatilization behavior [28]. The final temperature must be high enough for the complete decomposition of the carbonaceous materials. Finally, the heating rate is an important parameter as it greatly affects the rate of release of the volatiles due to the thermal inertia of the particles, and, in this way, different heating rates should be applied in order to study its influence [29].

Non-isothermal experiments are generally adopted for the determination of kinetic parameters as they are considered more reliable and less time-consuming when compared with isothermal experiments [30]. Moreover, TGA is very useful in studying the kinetics of biomass combustion because it is a simple and effective way to obtain information on the processes taking place for determining the kinetic parameters [31–34]. Thus, non-isothermal experiments include information on the temperature dependence of the reaction rate, and it is commonly believed that this would be sufficient to derive Arrhenius parameters and the reaction model of a process [35]. Consequently, the heating rate is one of the most relevant parameters in TGA as it affects thermal decomposition and, usually, experiments need to be performed with different heating rates to resolve possible compensation effects [36].

Thus, the Kinetics Committee of the ICTAC recommends that no less than three different temperature programs should be applied to obtain quality kinetic data [37].

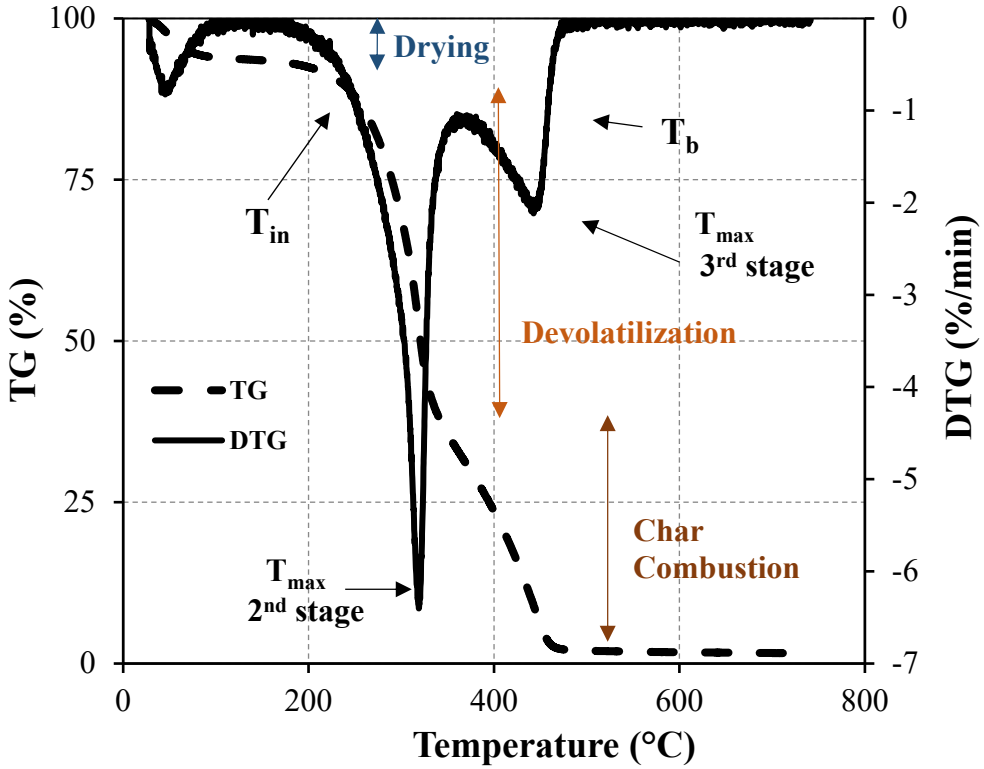

Figure 3. Mass loss as a function of time (above) and temperature (below) during the combustion of biomass [25].

The TGA results depend on several factors, but studies with a low heating rate are better at determining more precisely the temperatures from which the pyrolytic reactions start and avoiding transport effects [38]. In addition to the influence of the temperature and heating rate, Williams et al. [39] showed that the composition of the final products is dependent on the atmosphere. According to Vamvuka et al. [40], decreasing the oxygen concentration and increasing the particle size and moisture content will cause the ignition and burnout temperature to increase. Consequently, these variations will increase the residence time in the combustion chamber. Furthermore, Vamvuka et al. [40] reported that the composition of the gases, tars, and chars derived from biomass combustion depends on the heating rate and final temperature amongst other factors. Mani et al. [41] also investigated the influence of different parameters and found that the curves corresponding to the third stage of pyrolysis depend upon the particle size, initial weight, and heating rate of the pyrolysis process. Furthermore, an increase in the particle size and heating rate increases the char yield at the end of the experiments. Boriouchkine et al. [42] investigated the combustion of different particle sizes of spruce bark and wood residues. This study revealed that larger particles produced the highest maximum mass-loss rate when compared to smaller particles. Regarding the effect of the heating rate, Yorulmaz et al. [43] analyzed the combustion kinetics of treated and untreated waste wood using TGA under three different heating rates. This study revealed that by increasing the heating rate, the peak and burnout temperatures for all the samples were also increased, and higher temperatures were detected for the same weight loss. Shen et al. [44] examined the effect of the heating rate of four different biomass species, and the experimental results were used to develop a two-step reaction kinetic scheme with the activation energy depending on the heating rate. There have also been some studies that analyzed the effect of different heating rates on biomass decomposition under inert atmospheres [30,45–50]. However, as reported by Shen et al. [51] and Anca-Couce et al. [52], the presence of oxygen enhances biomass decom-

position and promotes char combustion. Furthermore, the kinetic parameters derived from oxidant environments differ remarkably from experiments in the absence of oxygen [53].

Furthermore, in a real application of biomass combustion to produce power, for instance in an industrial grate-fired boiler, the temperature of the biomass increases and volatiles are quickly released due to the high heating rate that they are exposed to (around 1 to 100 K/s) [54]. This fast reaction results in insufficient air diffusing into the biomass, and ambient oxygen concentration varies over time which means that the reaction will change from pyrolysis to combustion [55]. Although modern boilers operate with oxygen-limited combustion under a low primary air flow rate, it is important to point out that most of the time this equipment operates with reaction-limited combustion due to a high primary air supply [56]. However, most of the studies in the literature have investigated pyrolysis using inert atmospheres [40,44,46,47,57–64].This is due to the fact that pyrolysis is the first step in thermochemical processes such as combustion and gasification [64].

Few results have been generated from experiments with air [36,43,44,65–68]. Shen et al. [51] and Anca-Couce et al. [52] reported that the presence of oxygen enhances biomass decomposition and promotes char combustion. Furthermore, the kinetic parameters resulting from oxidative atmospheres differ significantly from those in experiments conducted in the absence of oxygen [52]. Therefore, to simulate combustion conditions, it is important to study thermal behavior and kinetics in an oxygen atmosphere. Thus, in order to understand these differences, the influence of both oxidative and non-oxidative atmospheres on biomass thermal conversion have been studied by different authors [24,51,69,70]. Munir et al. [69] analyze the thermal characteristics of four waste biomass materials and the results showed that it is a complex phenomenon due to different microstructural and elemental characteristics as well as the type of atmosphere. The authors found that the weight loss rate in an inert atmosphere was slower, and its reactivity was 52% to 77% less than in oxidative conditions. Similar results were reported more recently by Sher et al. [70] who assessed the thermal and kinetic behaviors of diverse biomass fuels to provide valuable information for the power generation industry.

Yuzbasi et al. [24] compared the pyrolysis and combustion of co-firing biomass and coal with the individual behavior of each solid fuel. Regarding pyrolysis, a similar trend was obtained up to 700 °C. Furthermore, the oxygen levels shift the combustion profile to lower temperatures and increase the weight loss rate.

Shen et al. [51] investigated the thermal degradation of pine and birch and applied a new kinetic model, the distributed activation energy model (DAEM). DAEM was found unsuitable to describe the thermal decomposition of biomass under oxidant conditions due to the capacity of oxygen to accelerate the mass loss in the first stage and promote complex reactions in the second stage. Furthermore, some works analyzed the influence of oxidant and non-oxidant environments through experiments with different oxygen concentrations [28,55,71–73].

Fang et al. [55] studied the effects of oxygen concentration on the mass-loss rate and kinetics of pyrolysis and combustion of wood. The author stated that the mass-loss rates of wood were independent of oxygen concentration when the temperature was below 250 °C. Furthermore, it was found that the activation energy varied linearly with oxygen concentration at the first stage. Moreno et al. [73] also studied the kinetics of wood wastes and solid wood under different conditions examining three or four reactions with regards to whether the reaction occurred under oxidative or non-oxidative conditions. In turn, Amutio et al. [72] proposed a kinetic model consisting of six simultaneous reactions.

Chouchene et al. [71] studied the effect of three atmospheres with different oxygen content on the thermal degradation of solid waste. It was verified that pyrolysis under inert conditions takes place according to two different stages (drying and devolatilization) while under oxidative conditions a third stage, char oxidation, occurs. On the other hand, Su et al. [28] analyzed the effect of oxygen content on the thermal degradation of pine and similar results were obtained. The oxygen promoted the degradation of biomass, and a third stage was observed.

While the previous literature has cast light on TGA under a variety of conditions, only a few works have succeeded in analyzing thermal conversion, and determining all the kinetic parameters of experiments covering the possibility of oxidative and non-oxidative conditions with different flow rates. To date, several studies have considered these different parameters, including particle size [40–42] and heating rate [30,36,43–52,74–80], while studying their influence on thermal degradation behavior and kinetics. Additionally, in the literature, there are several kinetic data derived from the weight loss curves of biomass fuels in inert [29,41,42,46–48,50,60–62,79,81–86] and air [27,36,43,66,67,87–89] atmospheres. There are also other investigations that have studied the influence of the atmosphere and applied both atmospheres [24,28,51,55,69,70,73]. This extensive literature review concludes with the selection and analysis of works that analyzed the most representative solid biomass fuels (eucalyptus, acacia, and pine), which are summarized in Table 1.

Hence, considering the current state-of-the-art in this subject, many factors can affect the kinetic parameters, including not only the process conditions, heterogeneity of the sample, heat and mass transfer limitations, and systematic errors, but also the processing and method for the analysis of the TGA results [16]. Consequently, a wide range of kinetic parameters has been reported in the literature and, therefore, direct comparisons are not possible. As evidence of this inconsistency, Figure 4 presents the different activation energy values reported in the literature for pine devolatilization and char oxidation. The set of results show a wide dispersion of data, which can be by a factor of up to five, depending on the author. This clearly shows that further experimentation should be carried out using TG analysis for the determination of the activation energy at each step of the biomass conversion.

Table 1. Literature review of experimental works that used pine, acacia, and eucalyptus samples.

Author	Country	Reactor Model	Biomass Type	Surrounding Environment	Mass (mg)	Size (µm)	Final Temperature (K)	Heating Rate (K/min)	Kinetic Method
Xu et al. [90] 2021	China	SDTA851E	Pine	Air 60 mL/min	NA	<200	873	5 to 40	2-stage mechanism and OFW, Starink, DAEM, and CR
Chen et al. [91] 2020	China	SDTA851E	Pine needle	Air 100 mL/min	1.6	75–150	870	5 to 40	3-stage mechanism and OFW, KAS, and CR
Fu et al. [92] 2019	China	TA Instrument SDT Q600	Eucalyptus bark	N_2 100 mL/min	5–10	150–300	1073	10 to 30	Model-fitting
Vega et al. [93] 2019	Colombia	LINSEIS, STA PT-1600	Pine and Acacia	N_2/O_2 mixture 50/13 mL/min	10	mesh 30 and mesh 60	1173	5 to 15	OFW
Mishra et al. [30] 2018	India	Hitachi, TA-7000	Pine, sal sawdust, and areca nut husk	N_2 50 mL/min	8	<1000	1173	5 to 25	1-global, KAS, OFW, CR, FR and DAEM
Wadhwani et al. [94] 2017	Australia	Mettler Toledo TGA/DSC 1	Pine and eucalyptus	N_2 20 mL/min	7.5	1–4000	1173	5 to 100	1-global, KAS and OFW
Cai et al. [95] 2016	China	NETZSCH STA 409 PC	Eucalyptus and paper mill sludge	Air 200 mL/min	6	<200	1223	10 to 40	KAS and Starink
Álvarez et al. [74] 2016	Spain	Perkin Elmer STA 6000	28 different biomass samples	Air 40 mL/min	10	250–500	1173	5 to 20	2-stage reaction and KAS, OFW, CR
Yu et al. [75] 2016	China	TA Instruments, SDT Q-600	Eucalyptus bark	Air 100 mL/min	10	200–600	1223	10 to 20	2-stage reaction and OFW and CR
Soria-Verdugo et al. [76] 2015	Spain	TA Instruments Q-500	Pine, olive kernel, thistle flower, and corncob	N_2 60 mL/min	10	<100	1073	10 to 40	DAEM
Soria-Verdugo et al. [76] 2015	Spain	TA Instruments Q-500	Pine, olive kernel, thistle flower, and corncob	N_2 60 mL/min	10	<100	1073	10 to 40	DAEM
Chen et al. [77] 2015	China	Pyris1 TGA Instrument	Eucalyptus leaves, bark, and sawdust	Ar 100 mL/min	5	74	1073	5 to 50	DAEM
Mishra et al. [49] 2015	India	DTG-60 unit	Pine	N_2 100 mL/min	10	50	973	5 to 40	OFW, KAS, FR, VY, VY AIC, and z(α) master plots
Saldarriaga et al. [63] 2015	Spain	TA Instruments Q-500	Pine	N_2 60 mL/min	10	<100	873	3 to 200	DAEM
Soria-Verdugo et al. [78] 2014	Spain	TA Instruments Q-500	Pine	N_2 60 mL/min	10	<100	873	3 to 200	DAEM

Table 1. *Cont.*

Author	Country	Reactor Model	Biomass Type	Surrounding Environment	Mass (mg)	Size (μm)	Final Temperature (K)	Heating Rate (K/min)	Kinetic Method
Fang et al. [96] 2013	China	Mettler Toledo TGA/SDTA851	Pine	Air 60 mL/min	10	<2000	773	30	1-global, CR
Anca-Couce et al. [52] 2012	Germany	Linseis Thermal Analysis, L81/1000	Pine	N_2 and O_2	2–4	200	873	2.5 to 10	FR, KAS, and Fitting algorithm
Amutio et al. [72] 2012	Spain	TA Instruments Q5000	Pine	N_2 and O_2 100 mL/min	10	<200	1073	15	Optimization model
Shen et al. [51] 2011	United Kingdom	TGA Mettler Toledo TGA/SDTA 8951E	Pine	N_2/Air 50 mL/min	<5	<300	1173	5 to 30	1-global, CR and DAEM
Kim et al. [45] 2010	Republic of Korea	TA Instruments, Q-50	Pine	N_2 20 mL/min	25	600 and 850	1073	5 to 50	Differential method
Shen et al. [44] 2009	United Kingdom	TGA Mettler Toledo TGA/SDTA 8951E	Pine	Air 60 mL/min	<5	500	1073	5 to 50	2-stage reaction, CR
Lapuerta et al. [97] 2007	Spain	TGA Seiko Instruments 6200	Pine	N_2 100 mL/min	10	<50	1100	5 to 40	Fitting algorithm
Lapuerta et al. [98] 2004	Spain	TGA Seiko Instruments 6200	Pine	N_2 50 mL/min	10	<500	1100	10 to 60	Fitting algorithm
Gronli et al. [59] 2002	Norway	TA Instruments SDT 2960	Pine	N_2 150 mL/min	5	NA	773	5	Optimization model
Bilbao et al. [65] 1997	Spain	SETARAM 92	Pine	Air 100 mL/min	3 and 20	630	≈1023	7 and 12	NA

CR—Coats Redfern. DAEM—Discrete Activation Energy Model. KAS—Kissinger-Akahira-Sunose. NA—Not Available. OFW—Ozawa-Flynn-Wall. TA—Thermogravimetric Analyzer. Vy—Vyazovkin.

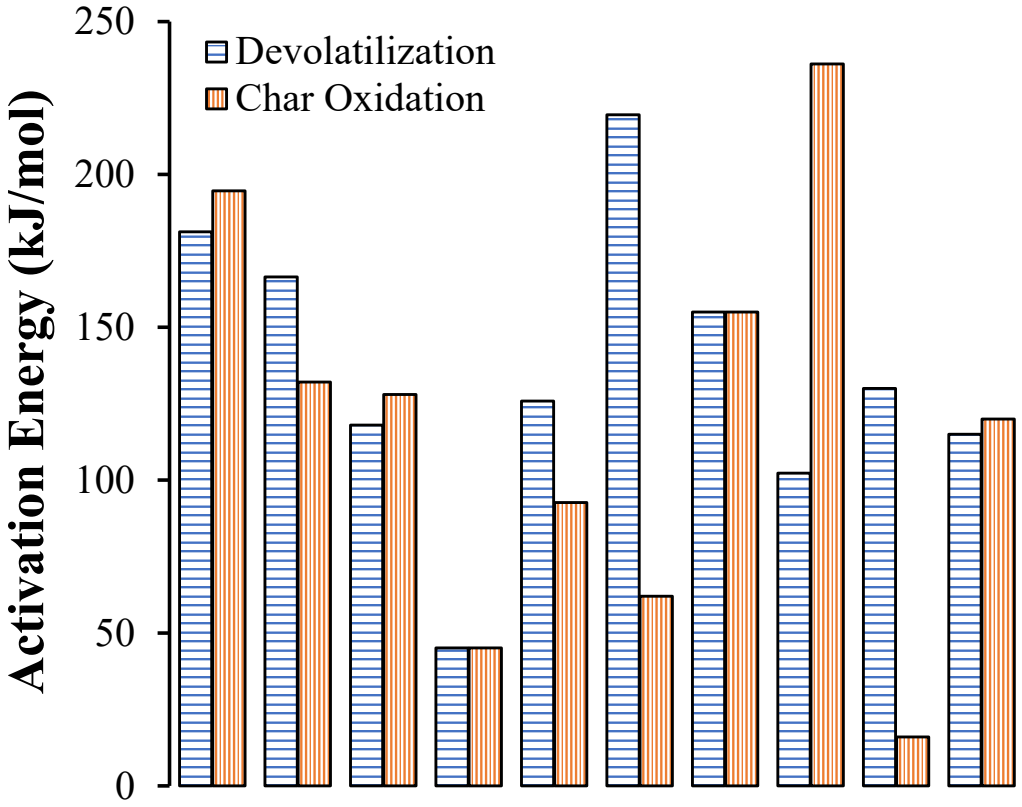

Figure 4. Activation energy values reported in the literature for pine devolatilization and char oxidation using two-step sequential models. The red bars are results considering a global reaction. Data Source: [43,44,51,72,74,90,91,96,99].

2.2. Macro Thermogravimetric Analysis

Experiments in a lab-scale reactor are an interesting alternative to address the biomass conversion in a real scale, and also to provide complementary knowledge to the TGA results about the kinetics of the reaction in the thermal biomass decomposition. This is also particularly interesting because the conditions in biomass industrial boilers are different, and it is important to investigate the thermal decomposition of larger particles and higher biomass quantities than those possible with TGA experiments. This possibility will allow us to take into consideration the heat and mass diffusion in the reaction mechanism. Furthermore, using larger samples, the effects of secondary reactions together with the possibility of operating at higher heating rates can also affect the reaction kinetics. Consequently, due to the complexity of the combustion process inside industrial boilers, which is enhanced with the motion of the fuel bed, there are several authors that report experiments in a batch reactor in order to describe the entire process in a traveling or vibrating grate boiler [100–105]. These experiments often include the combustion of a large amount of biomass (in the range of a number of kilograms). Experiments using batch reactors are also performed to quantify the implications of differences in fuel properties, and to investigate the propagation of a combustion front, i.e., the drying, pyrolysis, and char combustion process, in a bed of biomass particles. Such experiments are useful to develop parametric studies with different operating conditions (primary and secondary air flow rate and temperature) and different fuel properties (moisture content, volatile matter, ash content, chemical composition, heating values, and particle size). The ignition front velocity, ignition rate, conversion rate, and temperature of the reaction zone are the parameters most commonly obtained to evaluate combustion behavior.

Unlike this type of experiment, macro-TGA experiments are a simple and effective technique that allows to particularly study a higher biomass quantity, with a particle size representative of the fuel used in industrial facilities, in a small reactor. The reactors are then connected to a system to provide insight into the devolatilization products. Table 2 presents an overview of the macro-TGA studies presented in the literature. Only investigations considering combustion and pyrolysis experiments in isothermal conditions were considered in order to approximate the typical operating conditions of a grate furnace.

Thus, macro-TGA experiments provide the ability to control and maintain external heat fluxes, in order to better represent at small scale the conditions of industrial boilers when compared to horizontal or lamp tube reactors presented in the literature [106].

Table 2. Isothermal combustion and pyrolysis studies using the macro-TGA technique.

Author	Fuel	Temperature (°C)	Flow Rate (L/min)	Mass (g)	Particle Size (mm)	Gas Analysis
Hu et al. [107] 2021	Pellets	600 to 900	Different atmospheres, 0.1	0.4	8	MS
Nikku et al. [108] 2019	MSW, biomass, and coal	700, 800, 900	Reduced O_2, 3	0.1	4	FTIR
Baumgarten et al. [109] 2019	Oak and Spruce	250 to 450	Air, NA	1	<2	Not measured
Samuelsson et al. [110] 2017	Spruce	300 to 400	N_2, 7	0.16–0.69	15–24	Not measured
Orang et al. [111] 2015	Cedar, Pine, Poplar, and Oak	400 to 800	Air, 1	1	15	Not measured
Brunner et al. [112] 2013	Beech, Spruce, Poplar, and Willow	450–750	Air, 30	147.4	Random	FTIR, NDIR, FID, CLD
Gauthier et al. [106] 2013	Beech	450 to 1050	N_2, 2	NA	20 × 30	Micro-GC and a FTIR
Bennadji et al. [113] 2013	Poplar	375, 418	N_2, NA	5.5	19 × 40	FTIR
Becidan et al. [114] 2007	Biomass Residues	600 to 900	N_2, 40	75	80–120	Micro-GC and a FTIR
Becidan et al. [115] 2007	Biomass Residues	600 to 900	N_2, 40	75	80–120	Not measured
Weissinger et al. [116] 2004	Fiberboard waste	300 to 800	Air, ≈2000	NA	NA	FTIR
Bruch et al. [117] 2003	Beech	500	N_2, NA	NA	8, 12 and 17	NA

CLD—Chemiluminescence Detector. FID—Flame Ionization Detector. FTIR—Fourier-transform infrared spectroscopy. GC—Gas Chromatography. MS—Mass Spectrometry. NDIR—Nondispersive Infrared Sensor.

3. Modelling Approaches to Biomass Conversion

Considering the laboratory-scale experiments mentioned above, there are some important and fundamental issues that should be addressed before the development of numerical models. Hence, issues like the mechanism that governs the biomass conversion, the determination of the reaction kinetics, and the quantification/modeling of the release of volatile gas are detailed in the following sub-sections.

3.1. Devolatilization Mechanisms

As biomass contains a high content of volatile matter, the description of the devolatilization process is essential. Devolatilization, often referred as pyrolysis, is a complex chemical process in which the particles decompose into different products including permanent gaseous compounds, tar, and char. Therefore, currently, there are two major issues in describing the devolatilization process. The first one is concerned with how the progress of biomass conversion can be represented, and the second one is related to how to properly determine the permanent gas released during the devolatilization.

Regarding the first issue, there are different methods in the literature for describing this step of biomass combustion. The kinetics of biomass combustion depend on many different factors, but the reaction mechanism/kinetic model influences the final result and the way the conversion of the biomass is considered to take place. According to earlier studies from Di Blasi [118] the kinetics of biomass conversion can be classified into three groups: (*i*) one-step global models, (*ii*) one-stage, multi-reaction models, and (*iii*) two-stage, semi-global models. However, in recent decades, as plenty of research has been published in the field of biomass combustion and pyrolysis, a kinetic description of the devolatilization mechanism has been provided for a better understanding. Thus, for the sake of simplicity and clarity, devolatilization and pyrolysis mechanisms can be essentially classified into four groups:

1. One-step global mechanism;
2. Multi-component parallel single reaction mechanism;
3. One-component competitive mechanism;
4. Detailed mechanisms.

These mechanisms assume two particular initial conditions: if biomass is considered as one component or a mixture of components, and if the devolatilization reaction is considered as a single reaction or a set of multiple competitive reactions. Consequently, the group is arranged from the simplest, the one-step global mechanism, to the more sophisticated and complex, the detailed mechanisms. The number of steps in each model refers to the number of kinetic pathways that the reaction can take.

The one-step global mechanism is the simplest decomposition mechanism, acceptable for most engineering applications requiring only mass-loss rate predictions [99,119–121], and can be easily obtained from traditional TGA analysis [122]. Secondary reactions are not included and the reaction products, as understood by most of the researchers [16], only consist of char and volatiles. Due to their simplicity, they are used in CFD models to represent and describe the coupled chemical, kinetic, and physical phenomena of the devolatilization process [67]. Equation (1) displays the form of the single-step mechanism. A second step is commonly added for char oxidation, as referred to in [45,48,49,74].

$$\text{Biomass} \rightarrow \text{Volatiles} + \text{Char} \quad (1)$$

The multi-component parallel single reaction mechanism represents biomass through its intrinsic components, and the devolatilization reaction is described as the sum of the contributions to the decomposition of each macromolecule. Equation (2) shows the main mechanism used in this category. The work of Gronli et al. [59] is one example where the devolatilization of different biomass species was predicted using this mechanism, which is considered more precise at predicting the mass-loss rate [119].

$$\begin{array}{c} \text{Cellulose} \rightarrow \text{Volatiles} + \text{Char} \\ \text{Hemicellulose} \rightarrow \text{Volatiles} + \text{Char} \\ \text{Lignin} \rightarrow \text{Volatiles} + \text{Char} \end{array} \quad (2)$$

In order to overcome the limitation of the first mechanism, the one-component competitive mechanism was introduced, and biomass competitively produces volatiles, tar, and char, as represented in Equation (3). As reviewed by Di Blasi [118], Shafizadeh and Chin [123] were the authors who introduced this model, and it is usually applied in fuel bed models [124]. This is a more comprehensive mechanism and requires deeper knowledge of the decomposition of biomass into the different products.

$$\begin{array}{c} \text{Biomass} \rightarrow \text{Volatiles} \\ \text{Biomass} \rightarrow \text{Tar} \\ \text{Biomass} \rightarrow \text{Char} \\ \text{Tar} \rightarrow \text{Volatiles} \\ \text{Tar} \rightarrow \text{Char} \end{array} \quad (3)$$

Detailed mechanisms, e.g., the Ranzi Model [125] and Shafizadeh and Bradbury model [126], are more comprehensive as they consider competitive and parallel reactions for multiple or intermediate components. In addition, these four types of different reaction schemes are classified as empirical or kinetic models [120]. Kinetic models are global devolatilization models and, essentially, the mass-loss rate is correlated with the temperature of the particle to determine the reaction rate which is expressed by an Arrhenius equation. The reaction rates are only valid for conditions with specific parameters, limiting their general applicability. A detailed description of these and other models used in the literature to describe biomass devolatilization is provided by White et al. [16], Branca et al. [127], and Várhegyi [128].

In addition to this category, there are network models which are very accurate in their predictions of devolatilization behavior, although they are computationally complex. The computational complexity of these network models, as it is considered the physicochemical description of the fuel, directly impacts the amount of time required to run complex simulations [7]. Hence some simulations use simple global devolatilization models instead of complex ones. However, global models generally do not apply to a range of coal types, heating rates, and temperatures as broad as network models, and therefore need to be optimized using trusted data or predictions. Although their origins lie in coal combustion, biomass devolatilization can be considered analogous to the same stage during the coal conversion, and the models have been adapted to biomass fuels. Models like the CPD (Chemical Percolation Devolatilization) [129], Bio-FLASHCHAIN [130], FG-DVC (Functional Group Depolymerization Vaporization Crosslinking) [131], and Kobayashi et al. [132] are examples of models developed for coal combustion which were subsequently converted to biomass (Bio-FG-DVC [133], Bio-FLASHCHAIN [134], and Bio-CPD [135]).

3.2. Reaction Kinetics

The fundamental basis of the kinetic models, that is essential for understanding and modeling the biomass combustion in furnaces, is the solid-state transformation rate from biomass to volatile products as is generally described in Equation (4):

$$\frac{d\alpha}{dt} = k\, f(\alpha) \quad (4)$$

where t is time (s), $f(\alpha)$ is a function called the reaction model which describes the dependence of the reaction model on the conversion rate (α), and k is the thermal dependence term (s^{-1}), that can be defined by the Arrhenius Equation (5):

$$k = A \exp\left(-\frac{E}{R\,T}\right) \quad (5)$$

Here, E is the activation energy (J/mol), T is the absolute temperature (K), R is the universal gas constant (J/mol·K), and A is the pre-exponential factor (s^{-1}). The former parameter means the minimum energy barrier required to break the bonds and change one chemical structure to another, while A is based on the collision theory and represents the number of collisions per unit of time occurring in the reaction.

Regarding the conversion rate (α), this term can be defined as a relation between the initial (m_0), final (m_f), and instantaneous (m_t) sample mass. It can be obtained from each thermogravimetric experiment, and it is defined in Equation (6):

$$\alpha = \frac{m_0 - m_t}{m_0 - m_f} \tag{6}$$

For non-isothermal experiments, at a constant heating rate ($\beta = dT/dt$), Equation (4) can be expressed as a function of temperature, yielding Equation (7):

$$\frac{d\alpha}{dT} = k\, f(\alpha) \frac{1}{\beta} \tag{7}$$

The experimental conditions and the reaction stage considered influence the reaction model. Generally, it is considered a first-order reaction, and this function can be expressed as $(1 - \alpha)$ [27,136]. Other functions commonly used if another reaction model is required are presented in Table 3.

Table 3. Solid-state rate expressions for the most common reaction mechanisms [16].

Model—Name of Functions		***f*(α)**	***g*(α)**
Reaction order controlled	Zero-order	1	α
	First-order	$(1-\alpha)$	$-\ln(1-\alpha)$
	nth order	$(1-\alpha)$	$(n-1)^{-1}(1-\alpha)^{(1-\alpha)}$
Diffusion	1-D	$1/2\alpha$	α^2
	2-D	$-\ln(\alpha-1)^{-1}$	$(1-\alpha)\ln(1-\alpha)+\alpha$
	Jander, 3-D	$1.5(1-\alpha)^{2/3}\left[1-(1-\alpha)^{1/3}\right]^{-1}$	$\left[1-(1-\alpha)^{1/3}\right]^2$
	Ginstiling-Brounshtein, 3-D	$0.5\left[(1-\alpha)^{-1/3}-1\right]^{-1}$	$1-2/3\alpha-(1-\alpha)^{2/3}$
Nucleation	Power law	$n\,\alpha^{(1-n^{-1})}$ n = 2/3, 1, 2, 3, 4	α^n n = 3/2, 1, 1/2, 1/3, 1/4
	Exponential law	$\ln\alpha$	α
	Avrami-Erofeev (n = 1, 2, 3, 4)	$n\,(1-\alpha)[-\ln(1-\alpha)]^{(1-n^{-1})}$	$-\ln(1-\alpha)^{n-1}$
	Prout-Tompkins	$\alpha\,(1-\alpha)$	$\ln\left[\alpha(1-\alpha)^{-1}\right]+C^{\alpha}$
Geometrical contraction	Contracting area (n = 2)	$1-(1-\alpha)^{1-n^{-1}}$	$1-(1-\alpha)^{n^{-1}}$
	Contracting volume (n = 3)	$(1-\alpha)^{1-n^{-1}}$	$1-(1-\alpha)^{n^{-1}}$

Integration constant.

With this reaction model, Equation (7) can be simplified as:

$$\frac{d\alpha}{(1-\alpha)} = \frac{A}{\beta}\exp\left(-\frac{E}{R\,T}\right)dT \tag{8}$$

The left side of Equation (8) is a function of the conversion rate, and the right side is a function of the temperature. Integrating both sides of Equation (8), Equation (9) is obtained:

$$g(\alpha) = \int_0^{\alpha} \frac{d\alpha}{(1-\alpha)} = \frac{A}{\beta}\cdot\int_{T_0}^{T}\exp\left(\frac{-E}{RT}\right)\cdot dT \tag{9}$$

Equation (9) has no exact solution and there are two main mathematical approaches to solve this equation and obtain the kinetics data from the thermogravimetric analysis: (1) model-free methods (isoconversional) and (2) model-based methods [36]. In order to avoid modeling complex reactions, model-free methods can be preferable since the chemical parameters are determined without using any specific reaction model [27].

There are many isoconversional kinetic methods including Friedman (FR) [137], Ozawa-Flynn-Wall (OFW) [138,139], Kissinger-Akahira-Sunose (KAS) [140–142], Starink [143], and Vyazovkin methods [144,145]. The corresponding equations and their advantages and disadvantages can be found in Table 4. In model fitting, different models such as the Coats-Redfern (CR) [146], Freeman and Carroll [147], Duvvuri et al. [148], and differential models, can be fitted to the experimental data and whichever generates the best statistical fit is selected to evaluate the kinetic parameters. An overview of the biomass characterization process to obtain the kinetic parameters is represented in Figure 5.

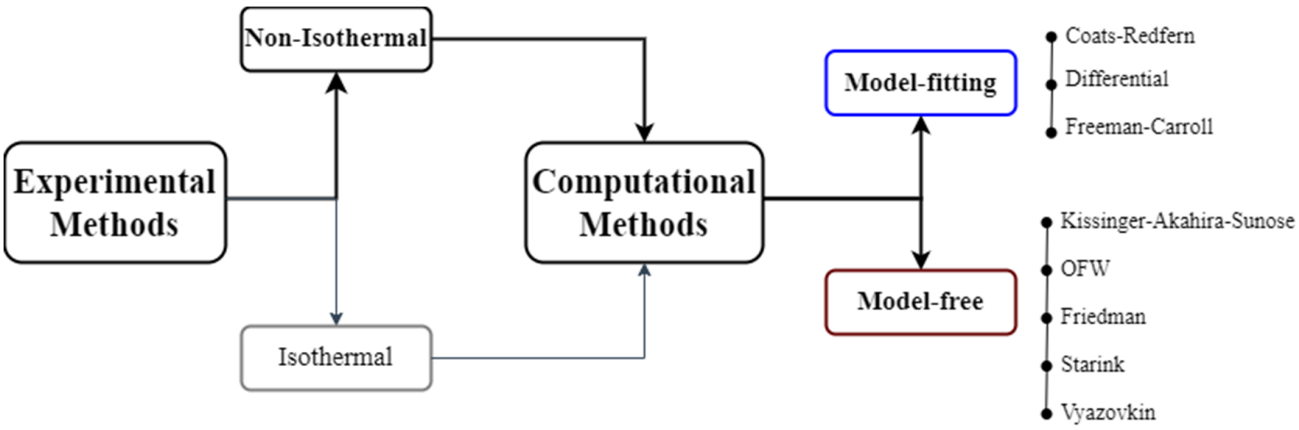

Figure 5. An overview of the methods for solid-state kinetics studies. Adapted from [151].

Table 4. Different kinetics methods used in the literature. Adapted from [149,150].

Method	Equation	E_α Determination (Slope of the Plots)	Advantages and Disadvantages
FR	$\ln\left[\beta_i\left(\frac{d\alpha}{dT}\right)_{\alpha,i}\right] = \ln[A_\alpha f(\alpha)] - \frac{E_\alpha}{RT_{\alpha,i}}$	$\ln\left[\beta_i\left(\frac{d\alpha}{dT}\right)_{\alpha,i}\right]$ vs. $\frac{-1}{RT_{\alpha,i}}$	Simple and Accurate; Numerically unstable and sensitive to data noise
OFW	$\ln\beta_i = \ln\left[\frac{A_\alpha E_\alpha}{Rg(\alpha)}\right] - 5.331 - 1.052\frac{E_\alpha}{RT_{\alpha,i}}$	$\ln\beta_i$ vs. $\frac{-1.052}{RT_{\alpha,i}}$	Oversimplified temperature integral
KAS	$\ln\left(\frac{\beta_i}{T^2_{\alpha,i}}\right) = \ln\left[\frac{A_\alpha R}{E_\alpha g(\alpha)}\right] - \frac{E_\alpha}{RT_{\alpha,i}}$	$\ln\left(\frac{\beta_i}{T^2_{\alpha,i}}\right)$ vs. $\frac{-1}{RT_{\alpha,i}}$	More accurate than OFW; Oversimplified temperature integral
Starink	$\ln\left(\frac{\beta_i}{T^{1.92}_{\alpha,i}}\right) = \text{Constant} - 1.008\frac{E_\alpha}{RT_{\alpha,i}}$	$\ln\left(\frac{\beta_i}{T^{1.92}_{\alpha,i}}\right)$ vs. $\frac{-1.0008}{RT_{\alpha,i}}$	More accurate temperature integral approximation
CR	$\ln\left[\frac{g(\alpha)}{T^2}\right] = \ln\left[\left(\frac{AR}{\beta E}\right)\left(1-\frac{2RT}{E}\right)\right] - \frac{E}{RT}$	$\ln\left[\frac{g(\alpha)}{T^2_\alpha}\right]$ vs. $\frac{-1}{RT_\alpha}$	Forcible fitting to reaction mechanism; Single values of E are obtained

However, the determination of the kinetic parameters for biomass thermal degradation is particularly complicated considering the presence of complex components and their consecutive and/or parallel reactions. The model-free method generates unique kinetic parameters as a function of the conversion rate since they are based on the principle that at each constant conversion the reaction rate is a function only of the temperature, such the one described in Equation (10) [152]:

$$\left[d\ln\left(\frac{d\alpha}{dt}\right)dT\right]_\alpha = [d\ln(k(T))dT]_\alpha + [d\ln(f(\alpha))dT]_\alpha \quad (10)$$

where α and $f(\alpha)$ are constant and, therefore, the second term on the right hand side of Equation (10) is zero. Hence, Equation (10) can be simplified to Equation (11):

$$\left[d\ln\left(\frac{d\alpha}{dt}\right)dT\right]_{\alpha} = \frac{-E_{\alpha}}{R} \tag{11}$$

Hence, this kinetic parameter is based on the evaluation of the dependence of the effective E on the conversion rate according to the TGA data from multiple heating rates, as suggested by the ICTAC [37]. The term effective is applied to emphasize the consequence of this dependency. Since in solid-state reactions the kinetic parameters may vary during the reaction progress, it is highly recommended to evaluate whether the E values remain constant to rule out the multi-step kinetic mechanism [151]. If E varies significantly, it means that the reaction process has more than one dominant reaction and a model-free type cannot be used for kinetic analysis. To overcome this problem, the CR method, a model-based method, is frequently applied by different researchers and produces similar E values to those calculated by model-free methods but depends on the selected reaction model considered [36]. The CR model uses the asymptotic series expansion for approximating the exponential integral in Equation (10). According to this model, the kinetic parameters can be determined by the equation presented in Table 4 and neglecting the term $2RT/E$, which can be considered much lower than one. The value for A is then determined from the interception of the plot indicated in Table 4 [153], with the possibility to make this analysis at different stages of the conversion process. Otherwise, to complete the determination of the kinetic parameters A and $f(\alpha)$, usually the Kissinger or compensation factor methods and master plots methods have been used to obtain both parameters, respectively [82].

Furthermore, post-processing TGA data is particularly important to obtain correct E values [150]. Consequently, there is a set of steps that should be considered, assessed, and implemented before the kinetic evaluation. Removal of the drying stage, floating points, and smoothing of the derivative conversion rate from the raw TGA data are common practice procedures, particularly if the FR method will be used. This method is different from the other isoconversional methods since the author uses the differential form of the Arrhenius equation, Equation (8), for the kinetic analysis. Thus, since no approximations or assumptions are used to solve the equation, it is considered more accurate than the other isoconversional methods, which are known as integral methods [149]. However, Mishra et al. [49] compared the E values from different isoconversional methods and observed higher values at the end of the conversion from the FR method. This means that the FR method is more dependent on the instantaneous conversion rate and more prone to experimental noise. This statement is in line with the findings of Starink [154].

3.3. Gas Release Quantification

A devolatilization mechanism and a kinetic model for mass loss describes the reaction that occurs during this stage but does not predict the gases released from the particles. Precisely in this regard, less attention has been paid to predicting the gaseous products. This the second issue of the devolatilization mechanism and description of the devolatilization process; the composition of the volatiles in biomass combustion requires additional models. These can be derived from proximate and ultimate analysis data, like the model proposed by Thunman et al. [155] or Neves et al. [121], or based on elemental species and an enthalpy conservation equation (e.g., [119]). Thunman et al. [155] used a chemical balance of the main elements of biomass fuels—carbon, hydrogen, and oxygen elements—to derive the composition of the products released during the devolatilization. An empirical model composed of three mass balance equations and one energy balance equation, together with two empirical ratios, are proposed to obtain the mass fractions of six chemical compounds (C_6H_6, CO, CO_2, H_2O, H_2, CH_4). Neves et al. [121] present a comprehensive review of the pyrolysis process and the development of an empirical model for the volatiles' composition. The focus of this review was on the secondary pyrolysis of gases and the product distribution and composition and the factors influencing them. The permanent gas compounds

include a broad range of different species and compounds and can be grouped, mainly, into CO, CO_2, H_2, and CH_4, as well as other light hydrocarbons. This composition is influenced by the heating rate and the main compounds show similar trends for temperature dependency, although the formation of CO_2 with respect to temperature changes deviates from what is observed in the case of the other compounds [121]. Furthermore, it was found that at temperatures above 500 °C the yields of gaseous products strongly become temperature dependent, leading to a substantial increase in the CO mass fractions. This is considered a result of secondary reactions, which result in the decrease in the tar mass fraction due to the conversion to CH_4 as well. Furthermore, it is highlighted that there is no significant dependency on CO_2, which means that it is the main product of primary reactions. The same behavior was described by Mehrabian et al. [119] based on dedicated experiments and data collected from previous work. Secondary reactions of the volatiles are negligible at low temperatures, and most of the permanent gases result from biomass thermal degradation. Within the low temperature range, gases like CO, CO_2, and H_2O are the main permanent gas compounds, with low quantities of CH_4. As the temperature increases, secondary reactions occur and an increase in CO and CH_4 are attributed to the decrease of tar. Here, due to higher temperatures, the yields of the volatiles have a strong correlation with the temperature, and CO results from the conversion of 2/3 of the tar.

However, the effects of this type of approach can produce unrealistic results [19,156–158], and experimental measurements in a lab-scale reactor are an interesting alternative to address this problem. In these types of experiments, the volatiles from thermochemical conversion are detected mainly using gas chromatographs and spectrometers [159]. Gas chromatography (GC) is a novel technique for studying the compounds released and the principle of operation consists of the separation of the individual components of the mixture so that each component can individually be identified and quantified through a detector. First, the sample is inserted into the equipment where it is transported via a carrier gas through a column and, depending on the physical properties of the compounds, the time the sample takes to reach the detector varies. Then, an electronic signal is generated based on interaction with the compound. The main detectors for GC instruments are thermal conductivity detectors (TCD) which are non-destructive and are usually incorporated before another common detector: flame ionizing detectors (FID). Another highly specific GC detector used is the chemiluminescence detector (CLD). More details about the performance and characteristics of the common GC detectors can be found in Li et al. [160] and in Regmi and Agah [161]. Spectrophotometry is an analytical technique that also allows us to separate, detect, and quantify gaseous compounds, but it is based on the absorption of light of the different compounds or on the mass to charge ratio of an ionized molecule. In this technique, there are two different types of spectrometers [162]. The first is referred to as infrared spectroscopy, and the Fourier Transform Infrared Spectroscopic (FTIR) and Nondispersive Infrared Sensor (NDIR) are the most common spectroscopic sensors used as a gas detector. The difference lies in the range of wavelengths bands that can be measured [163]. The second technique, mass spectrometry, is known in the literature as a sensitive detection technique [164] and the most suitable [165] for gas analysis. In addition, it can overcome the limitation of FTIR in measuring homodiatomic species like H_2 [162]. As presented in Table 2, Becidan et al. [114] applied chromatography and spectrophotometry to study the gases released during the combustion of biomass residues. A fraction of the exhaust gases is collected and analyzed using an FTIR analyzer and a micro-GC. The FTIR was used to quantify CO_2, CO, CH_4, C_2H_2, and C_2H_4. The gas samples were also quantified online using a micro-gas chromatograph equipped with two TCD detectors and a double injector connected to two columns to separate and quantify CO_2 and hydrocarbons (CH_4, C_2H_2, C_2H_4, and C_2H_6), and the remaining gases H_2, O_2, CH_4, CO and N_2 in another column. Brunner et al. [112] and Gauthier et al. [106] also applied both techniques to analyze the NOx emissions, the release of ash, and the main gaseous species and tar, respectively. Additionally, Weissinger et al. [116] described the release of nitrogen compounds using FTIR spectroscopy. Both works refer to the importance of

the determination of nitrogen gaseous compounds and that may serve as input profiles for CFD simulations. Bennadji et al. [113] and Nikku et al. [108] measured the fractions of light species from pyrolysis at low temperatures and compared the reactivity of MSW with biomass and coal samples through the FTIR technique, respectively. Hu et al. [107] analyzed the influence of different atmospheres in the gaseous conversion using a mass spectrometer.

Although the quantification of the gaseous compounds released during the thermal conversion of biomass is not addressed, there are works in the literature where the conversion of biomass was analyzed separately through the macro-TGA technique. Baumgarten et al. [109] and Samuelson et al. [110] analyzed the combustion behavior under typical isothermal conditions in the start-up of furnaces. Orang et al. [111] observed the effect of moisture content on combustion behavior. The author highlighted the increase in the drying and ignition times with the increasing moisture content.

4. Concluding Remarks

Biomass combustion for heat and power has seen rapid progress in both research initiatives and in market-oriented applications. In the previous sections, details regarding the major issues and achievements in biomass combustion, their characterization, and the current state-of-the-art around the thermal analysis for combustion modeling from a micro to macro perspective. As it was noticed, grate firing systems are widely used in combustion due to their capability to burn a broad range of fuels and with the main principle being to transport the fuel along the full length of the grate provided by grate movements and thus being able to have enough space for burning the particles. The difficulties and costs in performing experiments highlight the increase in the interest and necessity for a CFD analysis. Furthermore, the advances and constant improvement of computer performance also contributed to the increased role of CFD applications. Despite the significant attention in this field, improvements are still needed to make the modeling of large-scale grate-fired boilers affordable. Since various simplifications and assumptions have to be made to simulate a complete combustion system, some recommendations can be identified based on this comprehensive review in order to develop experiments to provide useful information for numerical models. Biomass conversion on the grate plays a key role in the overall performance of grate-fired boilers (for instance, combustion efficiency, pollutant emissions, and deposition) and several simplifications are necessary to keep the model numerically efficient. For this purpose, a set of equations describing the heat and mass transfer and chemical reactions in the fuel bed on the grate are required. The numerical results should always be validated with experimental data. Experimental measurements are an important aspect as they can provide the operating conditions, which cannot deviate from the normal state, and will be important to validate the numerical model [156]. Despite these facts, some details of the grate-firing systems are not readily accessible and uncertainty around the details in biomass-fired grate boilers challenge the modeling, operation, optimization, and, mainly, the validation of the numerical model. Phenomena such as combustion instabilities in the fuel bed (local burnouts, channeling formation, and spatially uneven fuel-bed thickness); non-continuous biomass feeding and grate movement; and irregular deposits on the furnace walls and air nozzles have to be considered when experimental measurements are being conducted to validate the numerical model.

Unquestionably, simplifying premises cannot be avoided due to the complexity of the entire process, as there are many and different physical and chemical phenomena occurring at the same time, considering the survey of the previous literature, further research is required to better understand the complexity of biomass conversion on a grate-fired boiler. The main process occurring during the particle conversion is devolatilization, and it is specifically in this stage where there is the main drawback and stiffness of the main CFD models. It is necessary to know the composition, the amount of pyrolysis products in different thermal conditions in the reactor, and the reaction rate of the particles. A recent investigation mentioned that numerical prediction inside a grate-fired boiler depends on the devolatilization kinetics mechanism, and that can significantly affect the outputs from the

bed model [166]. Most of the CFD models usually employed biomass elemental composition and an enthalpy conservation equation or models like that of Thunman et al. [155] and Neves et al. [121] to determine the composition of pyrolysis products (e.g., [119]). However, this type of approach can produce unrealistic results. Therefore, there is a clear need to use TGA and macro-TGA techniques to gain a full insight into the devolatilization behavior of biomass. Both techniques provide complementary information about kinetic mechanisms involved in thermal decomposition and volatiles composition. Another alternative to define the composition of the flue gas is based on experimental measurements. However, experiments during the operation of industrial boilers are difficult and expensive to carry out and the alternative is to conduct experiments at certain temperatures in a small reactor and use these results for the simulations [11,116,167]. In addition to all these aspects, another important consideration about the final biomass conversion stage should also be mentioned: char oxidation. According to Haberle et al. [168], the kinetics of char conversion is one of the most significant uncertainties in biomass thermal conversion modeling. Additionally, char yield varies depending on the reaction temperature and the heating rate [169]. Char reaction is also limited by the transport of reactants/products, mainly by oxygen diffusion [170]. Consequently, a combination of kinetic rate and oxygen diffusion should be considered for successful modeling of this heterogeneous reaction. This fact strengthens the need to use TGA and macro-TGA techniques to not only fully characterize the devolatilization reaction but also to obtain more knowledge about char oxidation and further improve biomass thermal conversion modeling.

In conclusion, from this literature analysis it can be stated that by having a proper model describing the different phenomena associated with the conversion on the grate, an accurate numerical model can be achieved combining TGA and macro-TGA experiments.

Author Contributions: Conceptualization, J.S., S.T. and J.T.; methodology, J.S., S.T. and J.T.; investigation, J.S.; writing—original draft preparation, J.S., J.T. and S.T.; writing—review and editing, J.S., J.T. and S.T.; supervision, J.T. and S.T. All authors have read and agreed to the published version of the manuscript.

Funding: This work was supported by the Portuguese Foundation for Science and Technology (FCT) within the R&D Units Project Scope UIDB/00319/2020 (ALGORITMI), and R&D Units Project Scope UIDP/04077/2020 (MEtRICs).

Data Availability Statement: No new data were created in this study. Data sharing is not applicable to this article.

Acknowledgments: The first author would like to express his gratitude for the support given by the FCT through the PhD Grant SFRH/BD/130588/2017.

Conflicts of Interest: The authors declare no conflict of interest.

Nomenclature

A pre-exponential factor, min^{-1}
E activation energy, kJ/mol
k rate of the chemical reaction, min^{-1}
m mass, g
R universal gas contant, kJ/(mol·K)
t time, min^{-1}
T temperature, °C

Greek symbols

α conversion rate, -
β heating rate, °C/min

Subscripts and superscripts

0 initial
f final
t time

References

1. Saidur, R.; Abdelaziz, E.A.; Demirbas, A.; Hossain, M.S.; Mekhilef, S. A review on biomass as a fuel for boilers. *Renew. Sustain. Energy Rev.* **2011**, *15*, 2262–2289. [CrossRef]
2. Norton, M.; Baldi, A.; Buda, V.; Carli, B.; Cudlin, P.; Jones, M.B.; Korhola, A.; Michalski, R.; Novo, F.; Oszlányi, J.; et al. Serious mismatches continue between science and policy in forest bioenergy. *GCB Bioenergy* **2019**, *11*, 1256–1263. [CrossRef]
3. Bilgili, F.; Koçak, E.; Bulut, Ü.; Kuşkaya, S. Can biomass energy be an efficient policy tool for sustainable development? *Renew. Sustain. Energy Rev.* **2017**, *71*, 830–845. [CrossRef]
4. Cowie, A.; Cowie, A.; Junginger, M.; Ximenes, F. Response to Chatham House Report "Woody Biomass for Power and Heat: Impacts on the Global Climate". 2017, pp. 1–14. Available online: https://www.ieabioenergy.com/wp-content/uploads/2017/03/Chatham_House_response_supporting-doc.pdf (accessed on 16 September 2022).
5. Gustavsson, L.; Haus, S.; Ortiz, C.A.; Sathre, R.; Le Truong, N. Climate effects of bioenergy from forest residues in comparison to fossil energy. *Appl. Energy* **2015**, *138*, 36–50. [CrossRef]
6. Evans, A.; Strezov, V.; Evans, T.J. Sustainability considerations for electricity generation from biomass. *Renew. Sustain. Energy Rev.* **2010**, *14*, 1419–1427. [CrossRef]
7. Banja, M.; Sikkema, R.; Jégard, M.; Motola, V.; Dallemand, J.-F. Biomass for energy in the EU—The support framework. *Energy Policy* **2019**, *131*, 215–228. [CrossRef]
8. IEA. Net Zero by 2050—A Roadmap for the Global Energy Sector. 2021. Available online: https://iea.blob.core.windows.net/assets/deebef5d-0c34-4539-9d0c-10b13d840027/NetZeroby2050-ARoadmapfortheGlobalEnergySector_CORR.pdf (accessed on 16 September 2022).
9. Deloitte. Towards an Integrated Energy System: Assessing Bioenergy's Socio-Economic and Environmental Impact. 2022. Available online: https://bioenergyeurope.org/article/347-towards-an-integrated-energy-system-assessing-bioenergy-s-socio-economic-and-environmental-impact.html (accessed on 16 September 2022).
10. Goyal, H.; Seal, D.; Saxena, R. Bio-fuels from thermochemical conversion of renewable resources: A review. *Renew. Sustain. Energy Rev.* **2008**, *12*, 504–517. [CrossRef]
11. Di Blasi, C.; Branca, C.; Santoro, A.; Gonzalez Hernandez, E. Pyrolytic behavior and products of some wood varieties. *Combust. Flame* **2001**, *124*, 165–177. [CrossRef]
12. Gil, L.; Bernardo, J. An approach to energy and climate issues aiming at carbon neutrality. *Renew. Energy Focus* **2020**, *33*, 37–42. [CrossRef]
13. Nussbaumer, T. Combustion and Co-combustion of Biomass: Fundamentals, Technologies, and Primary Measures for Emission Reduction. *Energy Fuels* **2003**, *17*, 1510–1521. [CrossRef]
14. Richardson, M.J. Thermal Analysis. In *Comprehensive Polymer Science and Supplements*; Elsevier: Amsterdam, The Netherlands, 1989; pp. 867–901. [CrossRef]
15. Vyazovkin, S.; Chrissafis, K.; Di Lorenzo, M.L.; Koga, N.; Pijolat, M.; Roduit, B.; Sbirrazzuoli, N.; Suñol, J.J. ICTAC Kinetics Committee recommendations for collecting experimental thermal analysis data for kinetic computations. *Thermochim. Acta* **2014**, *590*, 1–23. [CrossRef]
16. White, J.E.; Catallo, W.J.; Legendre, B.L. Biomass pyrolysis kinetics: A comparative critical review with relevant agricultural residue case studies. *J. Anal. Appl. Pyrolysis* **2011**, *91*, 1–33. [CrossRef]
17. Fernandez, A.; Soria, J.; Rodriguez, R.; Baeyens, J.; Mazza, G. Macro-TGA steam-assisted gasification of lignocellulosic wastes. *J. Environ. Manag.* **2019**, *233*, 626–635. [CrossRef]
18. Williams, A.; Jones, J.; Ma, L.; Pourkashanian, M. Pollutants from the combustion of solid biomass fuels. *Prog. Energy Combust. Sci.* **2012**, *38*, 113–137. [CrossRef]
19. Silva, J.; Teixeira, J.; Teixeira, S.; Preziati, S.; Cassiano, J. CFD Modeling of Combustion in Biomass Furnace. In *Energy Procedia*; Elsevier: Amsterdam, The Netherlands, 2017; pp. 665–672. [CrossRef]
20. Silva, J.; Fraga, L.; Ferreira, M.E.; Chapela, S.; Porteiro, J.; Teixeira, S.F.C.F.; Teixeira, J. Combustion Modelling of a 20 kW Pellet Boiler. In *Volume 6B Energy*; American Society of Mechanical Engineers: New York, NY, USA, 2018; p. V06BT08A036. [CrossRef]
21. Biagini, E.; Guerrini, L.; Nicolella, C. Development of a variable activation energy model for biomass devolatilization. *Energy Fuels* **2009**, *23*, 3300–3306. [CrossRef]
22. Fraga, L.; Silva, J.; Soares, D.F.; Ferreira, M.; Teixeira, S.F.; Teixeira, J.C. Study of Devolatilization Rates of Pine Wood and Mass Loss of Wood Pellets. In *ASME 2017 International Mechanical Engineering Congress and Exposition Volume 6 Energy*; ASME: Tampa, FL, USA, 2017; p. 9. [CrossRef]
23. Gil, M.; Casal, D.; Pevida, C.; Pis, J.; Rubiera, F. Thermal behaviour and kinetics of coal/biomass blends during co-combustion. *Bioresour. Technol.* **2010**, *101*, 5601–5608. [CrossRef]
24. Yuzbasi, N.S.; Selçuk, N. Air and oxy-fuel combustion characteristics of biomass/lignite blends in TGA-FTIR. *Fuel Process. Technol.* **2011**, *92*, 1101–1108. [CrossRef]
25. Fraga, L.G.; Silva, J.; Teixeira, J.C.F.; Ferreira, M.E.C.; Soares, D.F.; Teixeira, S.F. The effect of the heating and air flow rate on the mass loss of pine wood particles. In Proceedings of the 31st International Conference on Efficiency, Cost, Optimization, Simulation and Environmental Impact of Energy Systems, Guimarães, Portugal, 17–22 June 2018.
26. Jenkins, B.M.; Baxter, L.L.; Miles, T.R., Jr.; Miles, T.R. Combustion properties of biomass. *Fuel Process. Technol.* **1998**, *54*, 17–46. [CrossRef]

27. Magalhães, D.; Kazanç, F.; Riaza, J.; Erensoy, S.; Kabaklı; Chalmers, H. Combustion of Turkish lignites and olive residue: Experiments and kinetic modelling. *Fuel* **2017**, *203*, 868–876. [CrossRef]
28. Su, Y.; Luo, Y.; Wu, W.; Zhang, Y.; Zhao, S. Characteristics of pine wood oxidative pyrolysis: Degradation behavior, carbon oxide production and heat properties. *J. Anal. Appl. Pyrolysis* **2012**, *98*, 137–143. [CrossRef]
29. Saeed, M.; Andrews, G.; Phylaktou, H.; Gibbs, B. Global kinetics of the rate of volatile release from biomasses in comparison to coal. *Fuel* **2016**, *181*, 347–357. [CrossRef]
30. Mishra, R.K.; Mohanty, K. Pyrolysis kinetics and thermal behavior of waste sawdust biomass using thermogravimetric analysis. *Bioresour. Technol.* **2018**, *251*, 63–74. [CrossRef] [PubMed]
31. Skreiberg, A.; Skreiberg; Sandquist, J.; Sørum, L. TGA and macro-TGA characterisation of biomass fuels and fuel mixtures. *Fuel* **2011**, *90*, 2182–2197. [CrossRef]
32. Magdziarz, A.; Wilk, M. Thermogravimetric study of biomass, sewage sludge and coal combustion. *Energy Convers. Manag.* **2013**, *75*, 425–430. [CrossRef]
33. Grammelis, P.; Basinas, P.; Malliopoulou, A.; Sakellaropoulos, G. Pyrolysis kinetics and combustion characteristics of waste recovered fuels. *Fuel* **2009**, *88*, 195–205. [CrossRef]
34. Biswas, S.; Choudhury, N.; Sarkar, P.; Mukherjee, A.; Sahu, S.; Boral, P.; Choudhury, A. Studies on the combustion behaviour of blends of Indian coals by TGA and Drop Tube Furnace. *Fuel Process. Technol.* **2006**, *87*, 191–199. [CrossRef]
35. Vyazovkin, S.; Wight, C.A. Isothermal and non-isothermal kinetics of thermally stimulated reactions of solids. *Int. Rev. Phys. Chem.* **1998**, *17*, 407–433. [CrossRef]
36. Garcia-Maraver, A.; Perez-Jimenez, J.A.; Serrano-Bernardo, F.; Zamorano, M. Determination and comparison of combustion kinetics parameters of agricultural biomass from olive trees. *Renew. Energy* **2015**, *83*, 897–904. [CrossRef]
37. Vyazovkin, S.; Burnham, A.K.; Criado, J.M.; Pérez-Maqueda, L.A.; Popescu, C.; Sbirrazzuoli, N. ICTAC Kinetics Committee recommendations for performing kinetic computations on thermal analysis data. *Thermochim. Acta* **2011**, *520*, 1–19. [CrossRef]
38. Anca-Couce, A.; Tsekos, C.; Retschitzegger, S.; Zimbardi, F.; Funke, A.; Banks, S.; Kraia, T.; Marques, P.; Scharler, R.; de Jong, W.; et al. Biomass pyrolysis TGA assessment with an international round robin. *Fuel* **2020**, *276*, 118002. [CrossRef]
39. Williams, P.T.; Besler, S. The influence of temperature and heating rate on the slow pyrolysis of biomass. *Renew. Energy* **1996**, *7*, 233–250. [CrossRef]
40. Vamvuka, D.; Sfakiotakis, S. Combustion behaviour of biomass fuels and their blends with lignite. *Thermochim. Acta* **2011**, *526*, 192–199. [CrossRef]
41. Mani, T.; Murugan, P.; Abedi, J.; Mahinpey, N. Pyrolysis of wheat straw in a thermogravimetric analyzer: Effect of particle size and heating rate on devolatilization and estimation of global kinetics. *Chem. Eng. Res. Des.* **2010**, *88*, 952–958. [CrossRef]
42. Boriouchkine, A.; Sharifi, V.; Swithenbank, J.; Jämsä-Jounela, S.-L. A study on the dynamic combustion behavior of a biomass fuel bed. *Fuel* **2014**, *135*, 468–481. [CrossRef]
43. Yorulmaz, S.Y.; Atimtay, A.T. Investigation of combustion kinetics of treated and untreated waste wood samples with thermogravimetric analysis. *Fuel Process. Technol.* **2009**, *90*, 939–946. [CrossRef]
44. Shen, D.; Gu, S.; Luo, K.; Bridgwater, A.; Fang, M. Kinetic study on thermal decomposition of woods in oxidative environment. *Fuel* **2009**, *88*, 1024–1030. [CrossRef]
45. Kim, S.-S.; Kim, J.; Park, Y.-K. Pyrolysis kinetics and decomposition characteristics of pine trees. *Bioresour. Technol.* **2010**, *101*, 9797–9802. [CrossRef]
46. Seo, D.K.; Park, S.S.; Hwang, J.; Yu, T.-U. Study of the pyrolysis of biomass using thermo-gravimetric analysis (TGA) and concentration measurements of the evolved species. *J. Anal. Appl. Pyrolysis* **2010**, *89*, 66–73. [CrossRef]
47. Slopiecka, K.; Bartocci, P.; Fantozzi, F. Thermogravimetric analysis and kinetic study of poplar wood pyrolysis. *Appl. Energy* **2012**, *97*, 491–497. [CrossRef]
48. Chen, D.; Zheng, Y.; Zhu, X. In-depth investigation on the pyrolysis kinetics of raw biomass. Part I: Kinetic analysis for the drying and devolatilization stages. *Bioresour. Technol.* **2013**, *131*, 40–46. [CrossRef]
49. Mishra, G.; Kumar, J.; Bhaskar, T. Kinetic studies on the pyrolysis of pinewood. *Bioresour. Technol.* **2015**, *182*, 282–288. [CrossRef] [PubMed]
50. Wang, X.; Hu, M.; Hu, W.; Chen, Z.; Liu, S.; Hu, Z.; Xiao, B. Thermogravimetric kinetic study of agricultural residue biomass pyrolysis based on combined kinetics. *Bioresour. Technol.* **2016**, *219*, 510–520. [CrossRef] [PubMed]
51. Shen, D.; Gu, S.; Jin, B.; Fang, M. Thermal degradation mechanisms of wood under inert and oxidative environments using DAEM methods. *Bioresour. Technol.* **2011**, *102*, 2047–2052. [CrossRef]
52. Anca-Couce, A.; Zobel, N.; Berger, A.; Behrendt, F. Smouldering of pine wood: Kinetics and reaction heats. *Combust. Flame* **2012**, *159*, 1708–1719. [CrossRef]
53. Peters, B.; Raupenstrauch, H. Modeling Moving and Fixed Bed Combustion. In *Handbook of Combustion*; Wiley-VCH: Weinheim, Germany, 2010; p. 4. [CrossRef]
54. Kleinhans, U.; Wieland, C.; Frandsen, F.J.; Spliethoff, H. Ash formation and deposition in coal and biomass fired combustion systems: Progress and challenges in the field of ash particle sticking and rebound behavior. *Prog. Energy Combust. Sci.* **2018**, *68*, 65–168. [CrossRef]
55. Fang, M.; Shen, D.; Li, Y.; Yu, C.; Luo, Z.; Cen, K. Kinetic study on pyrolysis and combustion of wood under different oxygen concentrations by using TG-FTIR analysis. *J. Anal. Appl. Pyrolysis* **2006**, *77*, 22–27. [CrossRef]

56. Yin, C.; Rosendahl, L.A.; Kær, S.K. Grate-firing of biomass for heat and power production. *Prog. Energy Combust. Sci.* **2008**, *34*, 725–754. [CrossRef]
57. Xiao, R.; Yang, W.; Cong, X.; Dong, K.; Xu, J.; Wang, D.; Yang, X. Thermogravimetric analysis and reaction kinetics of lignocellulosic biomass pyrolysis. *Energy* **2020**, *201*, 117537. [CrossRef]
58. Flores, J.J.A.; Quiñones, J.G.R.; Rodríguez, M.L.; Vera, J.V.A.; Valencia, J.E.; Martínez, S.J.G.; Montesino, F.M.; Rosas, A.A. Thermal Degradation Kinetics and FT-IR Analysis on the Pyrolysis of Pinus pseudostrobus, Pinus leiophylla and Pinus montezumae as Forest Waste in Western Mexico. *Energies* **2020**, *13*, 969. [CrossRef]
59. Grønli, M.G.; Várhegyi, G.; Di Blasi, C. Thermogravimetric Analysis and Devolatilization Kinetics of Wood. *Ind. Eng. Chem. Res.* **2002**, *41*, 4201–4208. [CrossRef]
60. Saddawi, A.; Jones, J.M.; Williams, A.; Wójtowicz, M.A. Kinetics of the Thermal Decomposition of Biomass. *Energy Fuels* **2010**, *24*, 1274–1282. [CrossRef]
61. Darvell, L.; Jones, J.; Gudka, B.; Baxter, X.; Saddawi, A.; Williams, A.; Malmgren, A. Combustion properties of some power station biomass fuels. *Fuel* **2010**, *89*, 2881–2890. [CrossRef]
62. Parthasarathy, P.; Narayanan, K.S.; Arockiam, L. Study on kinetic parameters of different biomass samples using thermogravimetric analysis. *Biomass Bioenergy* **2013**, *58*, 58–66. [CrossRef]
63. Saldarriaga, J.F.; Aguado, R.; Pablos, A.; Amutio, M.; Olazar, M.; Bilbao, J. Fast characterization of biomass fuels by thermogravimetric analysis (TGA). *Fuel* **2015**, *140*, 744–751. [CrossRef]
64. Diblasi, C. Modeling chemical and physical processes of wood and biomass pyrolysis. *Prog. Energy Combust. Sci.* **2008**, *34*, 47–90. [CrossRef]
65. Bilbao, R.; Mastral, J.; Aldea, M.; Ceamanos, J. Kinetic study for the thermal decomposition of cellulose and pine sawdust in an air atmosphere. *J. Anal. Appl. Pyrolysis* **1997**, *39*, 53–64. [CrossRef]
66. Ren, X.; Chen, J.; Li, G.; Wang, Y.; Lang, X.; Fan, S. Thermal oxidative degradation kinetics of agricultural residues using distributed activation energy model and global kinetic model. *Bioresour. Technol.* **2018**, *261*, 403–411. [CrossRef]
67. Dhahak, A.; Bounaceur, R.; Le Dreff-Lorimier, C.; Schmidt, G.; Trouve, G.; Battin-Leclerc, F. Development of a detailed kinetic model for the combustion of biomass. *Fuel* **2019**, *242*, 756–774. [CrossRef]
68. Fraga, L.G.; Silva, J.; Teixeira, S.; Soares, D.; Ferreira, M.; Teixeira, J. Influence of Operating Conditions on the Thermal Behavior and Kinetics of Pine Wood Particles using Thermogravimetric Analysis. *Energies* **2020**, *13*, 2756. [CrossRef]
69. Munir, S.; Daood, S.; Nimmo, W.; Cunliffe, A.; Gibbs, B. Thermal analysis and devolatilization kinetics of cotton stalk, sugar cane bagasse and shea meal under nitrogen and air atmospheres. *Bioresour. Technol.* **2009**, *100*, 1413–1418. [CrossRef] [PubMed]
70. Sher, F.; Iqbal, S.Z.; Liu, H.; Imran, M.; Snape, C.E. Thermal and kinetic analysis of diverse biomass fuels under different reaction environment: A way forward to renewable energy sources. *Energy Convers. Manag.* **2020**, *203*, 112266. [CrossRef]
71. Chouchene, A.; Jeguirim, M.; Khiari, B.; Zagrouba, F.; Trouvé, G. Thermal degradation of olive solid waste: Influence of particle size and oxygen concentration. *Resour. Conserv. Recycl.* **2010**, *54*, 271–277. [CrossRef]
72. Amutio, M.; Lopez, G.; Aguado, R.; Artetxe, M.; Bilbao, J.; Olazar, M. Kinetic study of lignocellulosic biomass oxidative pyrolysis. *Fuel* **2012**, *95*, 305–311. [CrossRef]
73. Moreno, A.I.; Font, R.; Conesa, J.A. Combustion of furniture wood waste and solid wood: Kinetic study and evolution of pollutants. *Fuel* **2017**, *192*, 169–177. [CrossRef]
74. Álvarez, A.; Pizarro, C.; García, R.; Bueno, J.; Lavín, A. Determination of kinetic parameters for biomass combustion. *Bioresour. Technol.* **2016**, *216*, 36–43. [CrossRef]
75. Yu, D.; Chen, M.; Wei, Y.; Niu, S.; Xue, F. An assessment on co-combustion characteristics of Chinese lignite and eucalyptus bark with TG–MS technique. *Powder Technol.* **2016**, *294*, 463–471. [CrossRef]
76. Soria-Verdugo, A.; Goos, E.; García-Hernando, N. Effect of the number of TGA curves employed on the biomass pyrolysis kinetics results obtained using the Distributed Activation Energy Model. *Fuel Process. Technol.* **2015**, *134*, 360–371. [CrossRef]
77. Chen, Z.; Zhu, Q.; Wang, X.; Xiao, B.; Liu, S. Pyrolysis behaviors and kinetic studies on Eucalyptus residues using thermogravimetric analysis. *Energy Convers. Manag.* **2015**, *105*, 251–259. [CrossRef]
78. Soria-Verdugo, A.; Garcia-Gutierrez, L.; Blanco-Cano, L.; Garcia-Hernando, N.; Ruiz-Rivas, U. Evaluating the accuracy of the Distributed Activation Energy Model for biomass devolatilization curves obtained at high heating rates. *Energy Convers. Manag.* **2014**, *86*, 1045–1049. [CrossRef]
79. Kok, M.V.; Özgür, E. Thermal analysis and kinetics of biomass samples. *Fuel Process. Technol.* **2013**, *106*, 739–743. [CrossRef]
80. Granada, E.; Eguía, P.; Comesaña, J.A.; Patiño, D.; Porteiro, J.; Miguez, J.L. Devolatilization behaviour and pyrolysis kinetic modelling of Spanish biomass fuels. *J. Therm. Anal. Calorim.* **2013**, *113*, 569–578. [CrossRef]
81. Ghodke, P.; Mandapati, R.N. Investigation of particle level kinetic modeling for babul wood pyrolysis. *Fuel* **2019**, *236*, 1008–1017. [CrossRef]
82. Siddiqi, H.; Bal, M.; Kumari, U.; Meikap, B. In-depth physiochemical characterization and detailed thermo-kinetic study of biomass wastes to analyze its energy potential. *Renew. Energy.* **2019**, *148*, 756–771. [CrossRef]
83. Chen, J.; Wang, Y.; Lang, X.; Ren, X.; Fan, S. Evaluation of agricultural residues pyrolysis under non-isothermal conditions: Thermal behaviors, kinetics, and thermodynamics. *Bioresour. Technol.* **2017**, *241*, 340–348. [CrossRef]
84. Akinrinola, F.S.; Darvell, L.I.; Jones, J.M.; Williams, A.; Fuwape, J.A. Characterization of Selected Nigerian Biomass for Combustion and Pyrolysis Applications. *Energy Fuels* **2014**, *28*, 3821–3832. [CrossRef]

85. Amutio, M.; Lopez, G.; Alvarez, J.; Moreira, R.; Duarte, G.; Nunes, J.; Olazar, M.; Bilbao, J. Pyrolysis kinetics of forestry residues from the Portuguese Central Inland Region. *Chem. Eng. Res. Des.* **2013**, *91*, 2682–2690. [CrossRef]
86. Biagini, E.; Fantei, A.; Tognotti, L. Effect of the heating rate on the devolatilization of biomass residues. *Thermochim. Acta* **2008**, *472*, 55–63. [CrossRef]
87. Maia, A.A.D.; de Morais, L.C. Kinetic parameters of red pepper waste as biomass to solid biofuel. *Bioresour. Technol.* **2016**, *204*, 157–163. [CrossRef]
88. Aghamohammadi, N.; Sulaiman, N.M.N.; Aroua, M.K. Combustion characteristics of biomass in SouthEast Asia. *Biomass Bioenergy* **2011**, *35*, 3884–3890. [CrossRef]
89. Sanchez, M.; Otero, M.; Gómez, X.; Morán, A. Thermogravimetric kinetic analysis of the combustion of biowastes. *Renew. Energy* **2009**, *34*, 1622–1627. [CrossRef]
90. Xu, X.; Pan, R.; Chen, R. Combustion Characteristics, Kinetics, and Thermodynamics of Pine Wood Through Thermogravimetric Analysis. *Appl. Biochem. Biotechnol.* **2021**, *193*, 1427–1446. [CrossRef] [PubMed]
91. Chen, R.; Li, Q.; Xu, X.; Zhang, D.; Hao, R. Combustion characteristics, kinetics and thermodynamics of Pinus Sylvestris pine needle via non-isothermal thermogravimetry coupled with model-free and model-fitting methods. *Case Stud. Therm. Eng.* **2020**, *22*, 100756. [CrossRef]
92. Fu, S.; Chen, H.; Yang, J.; Yang, Z. Kinetics of thermal pyrolysis of Eucalyptus bark by using thermogravimetric-Fourier transform infrared spectrometry technique. *J. Therm. Anal. Calorim.* **2019**, *139*, 3527–3535. [CrossRef]
93. Vega, L.; López, L.; Valdés, C.F.; Chejne, F. Assessment of energy potential of wood industry wastes through thermochemical conversions. *Waste Manag.* **2019**, *87*, 108–118. [CrossRef] [PubMed]
94. Wadhwani, R.; Sutherland, D.; Moinuddin, K.A.M.; Joseph, P. Kinetics of pyrolysis of litter materials from pine and eucalyptus forests. *J. Therm. Anal. Calorim.* **2017**, *130*, 2035–2046. [CrossRef]
95. Cai, Z.; Ma, X.; Fang, S.; Yu, Z.; Lin, Y. Thermogravimetric analysis of the co-combustion of eucalyptus residues and paper mill sludge. *Appl. Therm. Eng.* **2016**, *106*, 938–943. [CrossRef]
96. Fang, X.; Jia, L.; Yin, L. A weighted average global process model based on two−stage kinetic scheme for biomass combustion. *Biomass Bioenergy* **2013**, *48*, 43–50. [CrossRef]
97. Lapuerta, M.; Hernández, J.J.; Rodríguez, J. Comparison between the kinetics of devolatilisation of forestry and agricultural wastes from the middle-south regions of Spain. *Biomass Bioenergy* **2007**, *31*, 13–19. [CrossRef]
98. Lapuerta, M.; Hernández, J.J.; Rodríguez, J. Kinetics of devolatilisation of forestry wastes from thermogravimetric analysis. *Biomass Bioenergy* **2004**, *27*, 385–391. [CrossRef]
99. Cancellieri, D.; Leroy-Cancellieri, V.; Silvani, X.; Morandini, F. New experimental diagnostics in combustion of forest fuels: Microscale appreciation for a macroscale approach. *Nat. Hazards Earth Syst. Sci.* **2018**, *18*, 1957–1968. [CrossRef]
100. Yang, Y.; Ryu, C.; Khor, A.; Sharifi, V.N.; Swithenbank, J. Fuel size effect on pinewood combustion in a packed bed. *Fuel* **2005**, *84*, 2026–2038. [CrossRef]
101. Ryu, C.; Yang, Y.B.; Khor, A.; Yates, N.E.; Sharifi, V.N.; Swithenbank, J. Effect of fuel properties on biomass combustion: Part I. Experiments—Fuel type, equivalence ratio and particle size. *Fuel* **2006**, *85*, 1039–1046. [CrossRef]
102. Mahmoudi, A.H.; Markovic, M.; Peters, B.; Brem, G. An experimental and numerical study of wood combustion in a fixed bed using Euler-Lagrange approach (XDEM). *Fuel* **2015**, *150*, 573–582. [CrossRef]
103. Wurzenberger, J.C.; Wallner, S.; Raupenstrauch, H.; Khinast, J.G. Thermal conversion of biomass: Comprehensive reactor and particle modeling. *AIChE J.* **2002**, *48*, 2398–2411. [CrossRef]
104. Markovic, M.; Bramer, E.A.; Brem, G. Experimental investigation of wood combustion in a fixed bed with hot air. *Waste Manag.* **2014**, *34*, 49–62. [CrossRef]
105. Erić, A.; Nemoda, S.; Komatina, M.; Dakić, D.; Repić, B. Experimental investigation on the kinetics of biomass combustion in vertical tube reactor. *J. Energy Inst.* **2019**, *92*, 1077–1090. [CrossRef]
106. Gauthier, G.; Melkior, T.; Grateau, M.; Thiery, S.; Salvador, S. Pyrolysis of centimetre-scale wood particles: New experimental developments and results. *J. Anal. Appl. Pyrolysis* **2013**, *104*, 521–530. [CrossRef]
107. Hu, Q.; He, X.; Yao, Z.; Dai, Y.; Wang, C.-H. Gaseous production kinetics and solid structure analysis during isothermal conversion of biomass pellet under different atmospheres. *J. Energy Inst.* **2021**, *98*, 53–62. [CrossRef]
108. Nikku, M.; Deb, A.; Sermyagina, E.; Puro, L. Reactivity characterization of municipal solid waste and biomass. *Fuel* **2019**, *254*, 115690. [CrossRef]
109. Baumgarten, B.; Reinhardt, J.; Lepski, C.; Risio, B.; Thorwarth, H. Kinetics of Wood Devolatilization during Start-up. *Energy Fuels* **2019**, *33*, 11285–11291. [CrossRef]
110. Samuelsson, L.N.; Umeki, K.; Babler, M.U. Mass loss rates for wood chips at isothermal pyrolysis conditions: A comparison with low heating rate powder data. *Fuel Process. Technol.* **2017**, *158*, 26–34. [CrossRef]
111. Orang, N.; Tran, H. Effect of feedstock moisture content on biomass boiler operation. *TAPPI J.* **2015**, *14*, 629–637. [CrossRef]
112. Brunner, T.; Biedermann, F.; Kanzian, W.; Evic, N.; Obernberger, I. Advanced Biomass Fuel Characterization Based on Tests with a Specially Designed Lab-Scale Reactor. *Energy Fuels* **2013**, *27*, 5691–5698. [CrossRef]
113. Bennadji, H.; Smith, K.; Shabangu, S.; Fisher, E.M. Low-Temperature Pyrolysis of Woody Biomass in the Thermally Thick Regime. *Energy Fuels* **2013**, *27*, 1453–1459. [CrossRef]

114. Becidan, M.; Skreiberg; Hustad, J.E. Products distribution and gas release in pyrolysis of thermally thick biomass residues samples. *J. Anal. Appl. Pyrolysis* **2007**, *78*, 207–213. [CrossRef]
115. Becidan, M.; Skreiberg; Hustad, J.E. Experimental study on pyrolysis of thermally thick biomass residues samples: Intra-sample temperature distribution and effect of sample weight ("scaling effect"). *Fuel* **2007**, *86*, 2754–2760. [CrossRef]
116. Weissinger, A.; Fleckl, T.; Obernberger, I. In situ FT-IR spectroscopic investigations of species from biomass fuels in a laboratory-scale combustor: The release of nitrogenous species. *Combust. Flame* **2004**, *137*, 403–417. [CrossRef]
117. Bruch, C.; Peters, B.; Nussbaumer, T. Modelling wood combustion under fixed bed conditions. *Fuel* **2003**, *82*, 729–738. [CrossRef]
118. Di Blasi, C. Modeling and simulation of combustion processes of charring and non-charring solid fuels. *Prog. Energy Combust. Sci.* **1993**, *19*, 71–104. [CrossRef]
119. Mehrabian, R.; Shiehnejadhesar, A.; Scharler, R.; Obernberger, I. Multi-physics modelling of packed bed biomass combustion. *Fuel* **2014**, *122*, 164–178. [CrossRef]
120. Hameed, S.; Sharma, A.; Pareek, V.; Wu, H.; Yu, Y. A review on biomass pyrolysis models: Kinetic, network and mechanistic models. *Biomass Bioenergy* **2019**, *123*, 104–122. [CrossRef]
121. Neves, D.; Thunman, H.; Matos, A.; Tarelho, L.; Gómez-Barea, A. Characterization and prediction of biomass pyrolysis products. *Prog. Energy Combust. Sci.* **2011**, *37*, 611–630. [CrossRef]
122. Gu, T.; Yin, C.; Ma, W.; Chen, G. Municipal solid waste incineration in a packed bed: A comprehensive modeling study with experimental validation. *Appl. Energy* **2019**, *247*, 127–139. [CrossRef]
123. Shafizadeh, F.; Chin, P.P.S. *Thermal Deterioration of Wood*; ACS Publications: Washington, DC, USA, 1977; pp. 57–81. [CrossRef]
124. Dernbecher, A.; Dieguez-Alonso, A.; Ortwein, A.; Tabet, F. Review on modelling approaches based on computational fluid dynamics for biomass combustion systems. *Biomass Convers. Biorefinery* **2019**, *9*, 129–182. [CrossRef]
125. Ranzi, E.; Cuoci, A.; Faravelli, T.; Frassoldati, A.; Migliavacca, G.; Pierucci, S.; Sommariva, S. Chemical Kinetics of Biomass Pyrolysis. *Energy Fuels* **2008**, *22*, 4292–4300. [CrossRef]
126. Bradbury, A.G.W.; Sakai, Y.; Shafizadeh, F. A kinetic model for pyrolysis of cellulose. *J. Appl. Polym. Sci.* **1979**, *23*, 3271–3280. [CrossRef]
127. Branca, C.; Albano, A.; Di Blasi, C. Critical evaluation of global mechanisms of wood devolatilization. *Thermochim. Acta* **2005**, *429*, 133–141. [CrossRef]
128. Várhegyi, G. Aims and methods in non-isothermal reaction kinetics. *J. Anal. Appl. Pyrolysis* **2007**, *79*, 278–288. [CrossRef]
129. Grant, D.M.; Pugmire, R.J.; Fletcher, T.H.; Kerstein, A.R. Chemical model of coal devolatilization using percolation lattice statistics. *Energy Fuels* **1989**, *3*, 175–186. [CrossRef]
130. Niksa, S. Rapid coal devolatilization as an equilibrium flash distillation. *AIChE J.* **1988**, *34*, 790–802. [CrossRef]
131. Solomon, P.R.; Hamblen, D.G.; Carangelo, R.M.; Serio, M.A.; Deshpande, G.V. General model of coal devolatilization. *Energy Fuels* **1988**, *2*, 405–422. [CrossRef]
132. Kobayashi, H.; Howard, J.; Sarofim, A. Coal devolatilization at high temperatures. *Symp. Combust.* **1977**, *16*, 411–425. [CrossRef]
133. Niksa, S. Predicting the rapid devolatilization of diverse forms of biomass with bio-flashchain. *Proc. Combust. Inst.* **2000**, *28*, 2727–2733. [CrossRef]
134. Serio, M.A. *A Comprehensive Model of Biomass Pyrolysis*; U.S. Department of Agriculture: Washington, DC, USA, 1997.
135. Sheng, C.; Azevedo, J. Modeling biomass devolatilization using the chemical percolation devolatilization model for the main components. *Proc. Combust. Inst.* **2002**, *29*, 407–414. [CrossRef]
136. Bahng, M.-K.; Mukarakate, C.; Robichaud, D.J.; Nimlos, M.R. Current technologies for analysis of biomass thermochemical processing: A review. *Anal. Chim. Acta* **2009**, *651*, 117–138. [CrossRef]
137. Friedman, H.L. Kinetics of thermal degradation of char-forming plastics from thermogravimetry. Application to a phenolic plastic. *J. Polym. Sci. Part C Polym. Symp.* **1964**, *6*, 183–195. [CrossRef]
138. Ozawa, T. A New Method of Analyzing Thermogravimetric Data. *Bull. Chem. Soc. Jpn.* **1965**, *38*, 1881–1886. [CrossRef]
139. Flynn, J.H.; Wall, L.A. General treatment of the thermogravimetry of polymers. *J. Res. Natl. Bur. Stand. Sect. A Phys. Chem.* **1966**, *70A*, 487. [CrossRef]
140. Kissinger, H.E. Variation of peak temperature with heating rate in differential thermal analysis. *J. Res. Natl. Bur. Stand* **1956**, *57*, 217–221. [CrossRef]
141. Kissinger, H.E. Reaction Kinetics in Differential Thermal Analysis. *Anal. Chem.* **1957**, *29*, 1702–1706. [CrossRef]
142. Akahira, T.; Sunose, T. Method of determining activation deterioration constant of electrical insulating materials. *Res Rep. Chiba Inst. Technol.* **1971**, *16*, 22–31.
143. Starink, M.J. The determination of activation energy from linear heating rate experiments: A comparison of the accuracy of isoconversion methods. *Thermochim. Acta* **2003**, *404*, 163–176. [CrossRef]
144. Vyazovkin, S.; Dollimore, D. Linear and Nonlinear Procedures in Isoconversional Computations of the Activation Energy of Nonisothermal Reactions in Solids. *J. Chem. Inf. Comput. Sci.* **1996**, *36*, 42–45. [CrossRef]
145. Vyazovkin, S. Modification of the integral isoconversional method to account for variation in the activation energy. *J. Comput. Chem.* **2001**, *22*, 178–183. [CrossRef]
146. Coats, A.W.; Redfern, J.P. Kinetic Parameters from Thermogravimetric Data. *Nature* **1964**, *201*, 68–69. [CrossRef]
147. Freeman, E.S.; Carroll, B. The Application of Thermoanalytical Techniques to Reaction Kinetics: The Thermogravimetric Evaluation of the Kinetics of the Decomposition of Calcium Oxalate Monohydrate. *J. Phys. Chem.* **1958**, *62*, 394–397. [CrossRef]

148. Duvvuri, M.S.; Muhlenkamp, S.P.; Iqbal, K.Z.W.J. Pyrolysis of natural fuels. *J. Fire Flammabl.* **1975**, *6*, 468–477.
149. Dhyani, V.; Bhaskar, T. Kinetic Analysis of Biomass Pyrolysis. In *Waste Biorefinery*; Elsevier: Amsterdam, The Netherlands, 2018; pp. 39–83. [CrossRef]
150. Cai, J.; Xu, D.; Dong, Z.; Yu, X.; Yang, Y.; Banks, S.W.; Bridgwater, A.V. Processing thermogravimetric analysis data for isoconversional kinetic analysis of lignocellulosic biomass pyrolysis: Case study of corn stalk. *Renew. Sustain. Energy Rev.* **2018**, *82*, 2705–2715. [CrossRef]
151. Khawam, A.; Flanagan, D.R. Basics and Applications of Solid-State Kinetics: A Pharmaceutical Perspective. *J. Pharm. Sci.* **2006**, *95*, 472–498. [CrossRef]
152. Vyazovkin, S.; Sbirrazzuoli, N. Isoconversional Kinetic Analysis of Thermally Stimulated Processes in Polymers. *Macromol. Rapid Commun.* **2006**, *27*, 1515–1532. [CrossRef]
153. Fraga, L.G.; Silva, J.; Teixeira, S.; Soares, D.; Ferreira, M.; Teixeira, J. Thermal Conversion of Pine Wood and Kinetic Analysis under Oxidative and Non-Oxidative Environments at Low Heating Rate. *Proceedings* **2020**, *58*, 23. [CrossRef]
154. Starink, M. A new method for the derivation of activation energies from experiments performed at constant heating rate. *Thermochim. Acta* **1996**, *288*, 97–104. [CrossRef]
155. Thunman, H.; Niklasson, F.; Johnsson, F.; Leckner, B. Composition of volatile gases and thermochemical properties of wood for modeling of fixed or fluidized beds. *Energy Fuels* **2001**, *15*, 1488–1497. [CrossRef]
156. Rahdar, M.H.; Nasiri, F.; Lee, B. A Review of Numerical Modeling and Experimental Analysis of Combustion in Moving Grate Biomass Combustors. *Energy Fuels* **2019**, *33*, 9367–9402. [CrossRef]
157. Silva, J.; Teixeira, J.; Teixeira, S.; Chapela, S.; Porteiro, J. Application of a biomass combustion model to an industrial boiler. In Proceedings of the 31st International Conference on Efficiency, Cost, Optimization, Simulation and Environmental Impact of Energy Systems, Guimarães, Portugal, 17–22 June 2018.
158. Silva, J.; Teixeira, J.; Teixeira, S.; Preziati, S. Analysis and Modeling of Combustion in Biomass Furnace. In Proceedings of the XXI Natl, Elche, Spain, 20 November 2016; p. 7.
159. Ong, H.C.; Chen, W.-H.; Singh, Y.; Gan, Y.Y.; Chen, C.-Y.; Show, P.L. A state-of-the-art review on thermochemical conversion of biomass for biofuel production: A TG-FTIR approach. *Energy Convers. Manag.* **2020**, *209*, 112634. [CrossRef]
160. Li, C.; Long, Z.; Jiang, X.; Wu, P.; Hou, X. Atomic spectrometric detectors for gas chromatography. *TrAC Trends Anal. Chem.* **2016**, *77*, 139–155. [CrossRef]
161. Regmi, B.P.; Agah, M. Micro Gas Chromatography: An Overview of Critical Components and Their Integration. *Anal. Chem.* **2018**, *90*, 13133–13150. [CrossRef]
162. Wang, S.; Dai, G.; Yang, H.; Luo, Z. Lignocellulosic biomass pyrolysis mechanism: A state-of-the-art review. *Prog. Energy Combust. Sci.* **2017**, *62*, 33–86. [CrossRef]
163. Zaharescu, M.; Mocioiu, O.C. Infrared Spectroscopy. In *Chemical Solution Deposition of Functional Oxide Thin Films*; Springer: Vienna, Austria, 2013; pp. 213–230. [CrossRef]
164. Huang, Y.; Kuan, W.; Chiueh, P.; Lo, S. Pyrolysis of biomass by thermal analysis–mass spectrometry (TA–MS). *Bioresour. Technol.* **2011**, *102*, 3527–3534. [CrossRef]
165. Radojević, M.; Janković, B.; Stojiljković, D.; Jovanović, V.; Čeković, I.; Manić, N. Improved TGA-MS measurements for evolved gas analysis (EGA) during pyrolysis process of various biomass feedstocks. Syngas energy balance determination. *Thermochim. Acta* **2021**, *699*, 178912. [CrossRef]
166. Jiang, M.; Lai, A.C.H.; Law, A.W.-K. Solid Waste Incineration Modelling for Advanced Moving Grate Incinerators. *Sustainability* **2020**, *12*, 8007. [CrossRef]
167. Ragland, K.; Aerts, D.; Baker, A. Properties of wood for combustion analysis. *Bioresour. Technol.* **1991**, *37*, 161–168. [CrossRef]
168. Haberle, I.; Skreiberg; Łazar, J.; Haugen, N.E.L. Numerical models for thermochemical degradation of thermally thick woody biomass, and their application in domestic wood heating appliances and grate furnaces. *Prog. Energy Combust. Sci.* **2017**, *63*, 204–252. [CrossRef]
169. Hoang, Q.N.; Vanierschot, M.; Blondeau, J.; Croymans, T.; Pittoors, R.; Van Caneghem, J. Review of numerical studies on thermal treatment of municipal solid waste in packed bed combustion. *Fuel Commun.* **2021**, *7*, 100013. [CrossRef]
170. Khodaei, H.; Al-Abdeli, Y.M.; Guzzomi, F.; Yeoh, G.H. An overview of processes and considerations in the modelling of fixed-bed biomass combustion. *Energy* **2015**, *88*, 946–972. [CrossRef]